ISSN: 0378-102X
www.ucm.es\JIG

Journal of Iberian Geology 30 (2004) 23-51

Journal of Iberian Geology
AN INTERNATIONAL PUBLICATION OF EARTH SCIENCES

The contact between the Ossa Morena and the South Portuguese zones. Characteristics and significance of the Aracena metamorphic belt, in its central sector between Aroche and Aracena (Huelva)

El contacto entre las zonas de Ossa Morena y Sudportuguesa. Características y significado de la banda metamórfica de Aracena, en su sector central entre Aroche y Aracena (Huelva)

M. Díaz Azpiroz[1], A. Castro[2], C. Fernández[3], S. López[2], J.C. Fernández Caliani[2], I. Moreno-Ventas[2]

[1]Depto. de Ciencias Ambientales, Univ. Pablo de Olavide. Carretera de Utrera, km 1. 41013 Sevilla, Spain.
[2]Depto. de Geología, Facultad de Ciencias Experimentales, Univ. de Huelva, Campus del Carmen, 21071 Huelva, Spain.
[3]Depto. de Geodinámica y Paleontología, Facultad de Ciencias Experimentales, Universidad de Huelva, Campus del Carmen, 21071 Huelva, Spain.

Received: 12/12/02 / Accepted: 05/12/03

Abstract

The boundary between the Ossa Morena and the South Portuguese zones is outlined by the Aracena metamorphic belt. The main characteristics of this region of the Iberian Massif are divided into lithologic, structural, metamorphic, magmatic, geochemical, isotopic and experimental points of view and presented in this paper. The Aracena metamorphic belt is divided into two main domains: the oceanic domain is composed of MORB-derived metabasites (the Acebuches metabasites) and a former accretionary prism. The continental domain comprises aluminous gneisses and migmatites, calc-silicate rocks, leucocratic gneisses, marbles, amphibolites, syn- to post-tectonic noritic intrusions with high-Mg andesite (boninitic affinities) composition, as well as post tectonic acid-to-basic intrusive rocks. The Acebuches metabasites were firstly affected by a high-temperature/low-pressure event, which currently shows an inverted metamorphic gradient, and is related to SW verging thrusting. The thermal peak related to this metamorphic event displays an age gradient in such a way that older ages have been obtained towards the west. The lower half of the Acebuches metabasite pile was later affected by a mylonitic deformation and a retrometamorphism related to the Southern Iberian Shear Zone. Four ductile deformation phases have been defined in the continental domain: CD-D_1 was related to the formation of km-scale recumbent folds. CD-D_2 could be associated with an extensional collapse or a gravity spreading, and is coeval with a high-temperature/low-pressure metamorphic event that affected the continental domain and gave place to several migmatitic complexes. CD-D_3 produced symmetric upright folds and CD-D_4 generated south-verging thrusts and thrusts accommodation folds.

The main characteristics of the Aracena metamorphic belt are interpreted as the result of a trench-trench-ridge triple junction evolution. According to the proposed model, the oceanic ridge-trench interaction led to the formation of a slab-free window beneath the continental margin, which provoked the upwelling of the underlying astenosphere and a subsequent thermal rebound. This triple junction migrated along the continental margin towards the east, which gave place to the generation of a high-temperature/low-pressure metamorphic belt in the contact between the Ossa Morena and the South Portuguese zones.

Keywords: Iberian Massif, Aracena metamorphic belt, shear deformation, HT/LP metamorphism, boninitic affinities, triple junction.

Corresponding author: Manuel Díaz Azpiroz, Tf: 34 954349161, Fax: 34 954349391, E-mail: mdiaazp@dex.upo.es

Resumen

El contacto entre las zonas de Ossa Morena y Sudportuguesa está subrayado por la banda metamórfica de Aracena. Las características principales de esta región del macizo Ibérico pueden considerarse desde distintos puntos de vista: litológico, estructural, metamórfico, magmático, geoquímica, isotópico y experimental, y así se presentan en este artículo. La banda metamórfica de Aracena está dividida en dos dominios principales: el dominio oceánico está formado por metabasitas derivadas de un MORB (las metabasitas de Acebuches) y por un antiguo prisma de acrección. El dominio continental incluye gneises y migmatitas alumínicos, rocas de silicatos cálcicos, gneises leucocráticos, mármoles, anfibolitas, intrusiones sin/post-tectónicas de noritas ricas en Mg (con afinidad boninítica), así como rocas intrusivas post-tectónicas de composición ácida a básica. Las metabasitas de Acebuches sufrieron, en primer lugar, un metamorfismo de alta temperatura/baja presión que, en la actualidad, presenta un gradiente metamórfico invertido, y que estaba relacionado con un cabalgamiento vergente al SO. El pico térmico asociado a este evento metamórfico muestra un gradiente de edad, de forma que las edades más antiguas han sido obtenidas en el extremo oeste. La mitad inferior de la pila metabasítica de Acebuches fue afectada posteriormente por una deformación milonítica y un retrometamorfismo asociados a la zona de cizalla Sudibérica. Cuatro fases de deformación dúctil han sido definidas en el dominio continental: la fase CD-D_1 estuvo relacionada con la generación de pliegues recumbentes de escala kilométrica. La fase CD-D_2 se puede asociar a un colapso extensional, y es contemporánea con un metamorfismo de alta temperatura/baja presión que afectó al dominio continental y generó diversos complejos migmatíticos. La fase CD-D_3 produjo pliegues simétricos verticales, mientras que la fase CD-D_4 dio lugar a cabalgamientos vergentes al sur a los que se asociaron pliegues de propagación.

Las principales características de la banda metamórfica de Aracena se interpretan como el resultado de la evolución de un punto triple de tipo fosa-fosa-dorsal. De acuerdo con el modelo propuesto, la interacción entre la dorsal y la zona de subducción dio como resultado la formación de una ventana astenosférica bajo el margen continental cabalgante, lo cual provocó el ascenso de la astenosfera y el consecuente rebote térmico. Esta unión triple migro a lo largo del margen continental hacia el este, lo que generó un cinturón metamórfico de alta temperatura/baja presión en el contacto entre las zonas de Ossa Morena y Sudportuguesa.

Palabras Clave: Macizo Ibérico, banda metamórfica de Aracena, deformación por cizalla, metamorfismo de AT/BP, afinidad boninítica, unión triple.

1. Introduction

The boundary between the Ossa-Morena Zone (OMZ) and the South Portuguese zone (SPZ), which are two of the main units of the Iberian Massif, is marked by the presence of a tectono-metamorphic terrain known as the Aracena metamorphic belt (AMB). Despite its regional significance, the AMB is not a well-known area within the Iberian Massif and few geologists have studied it so far. The AMB was first defined and divided into domains by Bard (1967a, b; 1969). These studies dealt mainly with geochemical and metamorphic features of the belt. Later on, several publications by Bard (1970; 1977), Bard and Moine (1979), Dupuy *et al.* (1979), Apalategui *et al.* (1983; 1984; 1990), Barranco *et al.* (1983), Munhá *et al.* (1986), Crespo-Blanc (1987; 1991), Crespo-Blanc and Orozco (1988; 1991), Abalos *et al.* (1991), Fonseca and Ribeiro (1993), Quesada *et al.* (1994) and Giese *et al.* (1994a, b) contributed to a better understanding of the structure and metamorphism in different areas of the AMB. Castro *et al.* (1996a, b), based on the main characteristics of the central sector of the AMB, proposed a model of triple junction evolution, including ridge subduction, for this sector of the Iberian Massif. Subsequent publications by Castro and co-workers have contributed to improve this model. As the area is possibly located at the edge of the Gondwana supercontinent, the proposed tectonic model may have implications in the understanding of the plate tectonic scenario during the Upper Palaeozoic. Moreover, studies dealing with the mineralogical, geochemical and metamorphic aspects of the calc-silicate series have been carried out by, among others, Rodas *et al.* (2000), Fernández-Caliani *et al.* (2001; 2002) and Moreno-Ventas *et al.* (2002).

The AMB has been revealed as an area of great geological interest. The oceanic domain of the AMB can be considered as the remnant of an old variscan ocean separating the OMZ and SPZ continental blocks (*e.g.*, Bard and Moine, 1979; Crespo-Blanc, 1991; Castro *et al.*, 1996b). It is, therefore, one of the scarce sutures observable in the Iberian Variscan belt. On the other hand, the occurrence of a high-temperature/low-pressure metamorphic event affecting the continental margin of the OMZ, as well as the early intrusion of noritic magmas with boninitic affinities, have been considered two remarkable features with relevant tectonic implications (Bard, 1969; Crespo-Blanc, 1991; Castro *et al.*, 1996a, b; 1999a; El-Biad, 2000; El-Hmidi, 2000; Díaz Azpiroz, 2001).

The AMB outcrops from Beja, in Portugal, to Almadén de la Plata, in the Seville province. Nevertheless, this paper will focus on the results arose from the latest studies carried out in the central sector (between the villages of Aroche and Aracena, in the Huelva province) of a high-grade band located at the southern boundary of the AMB. The mentioned studies comprise field, petrographic, mineral chemistry, whole-rock geochemistry and experimental petrology data, which have been dedicated to the analysis of structure, metamorphism, magmatism and isotope geochronology of the AMB. The present paper devotes a chapter to each of the subjects.

2. Regional setting and rock types of the Aracena metamorphic belt

The AMB is a high-grade metamorphic band, some tens of kilometres wide and more than 200 km long, whose limits lay parallel to the main regional structural trends, including the northern contact of the OMZ, which separates this unit from the Central Iberian zone (Fig. 1a). The AMB underwent a high-temperature/low-pressure (HT/LP) metamorphic event during the Variscan orogeny at the Upper Palaeozoic (*e.g.*, Castro *et al.*, 1996a, b; 1999a).

According to the division proposed by Castro *et al.* (1996a, b; 1999a), which is based on lithological, geochemical, metamorphic and structural features, two different domains can be distinguished in the AMB (Fig. 1b, c): a southern oceanic domain (OD), and a northern continental domain (CD). Two groups of rocks are distinguished in the OD. In the northern part, the Acebuches metabasites define a series of amphibolites and mafic schists which, according to several geochemical studies (Dupuy *et al.*, 1979; Munhá *et al.*, 1986; Quesada *et al.*, 1994; Castro *et al.*, 1996b), are the result of the metamorphism of a former oceanic crust with MORB affinities. To the south of the Acebuches metabasites is located the Pulo do Lobo terrain, that has been interpreted by Eden (1991) as a part of an old accretionary prism. On the other hand, the CD is formed mainly of pelitic gneisses and migmatites, calc-silicate rocks, leucocratic gneisses, amphibolites and marbles. In addition, syn- to late-tectonic intrusions of norites with boninitic affinities and post-tectonic plutons of gabbros, diorites and meta-aluminous granites have been described (Castro *et al.*, 1996b; El-Hmidi, 2000; Díaz Azpiroz, 2001; Díaz Azpiroz *et al.*, 2001). The CD has been divided, according to metamorphic grade criteria, into a northern medium-grade zone and a southern high-grade zone (Apalategui *et al.*, 1983; 1984; Crespo-Blanc, 1987; 1991; Castro *et al.*, 1999a; Díaz Azpiroz, 2001). The present paper will focus on the highest-grade areas of the AMB, which are the high-grade zone of the CD and the Acebuches metabasites of the OD.

As it will be shown later on in this paper, apart from composition, OD and CD are clearly separated according to their structural and metamorphic evolution. The CD was affected by a metamorphic event that shows an asymmetric zoning with the highest temperature zone located in the south edge, at the immediate contact with the OD (Castro *et al.*, 1996a, b). The peak assemblages show a post-tectonic growth with respect to the deformation phases responsible for the main fabrics in the CD. Later folding and shearing episodes affect the metamorphic isogrades. In the OD the metamorphic grade increases towards the structural top (*i.e.* opposite to the metamorphic zoning in

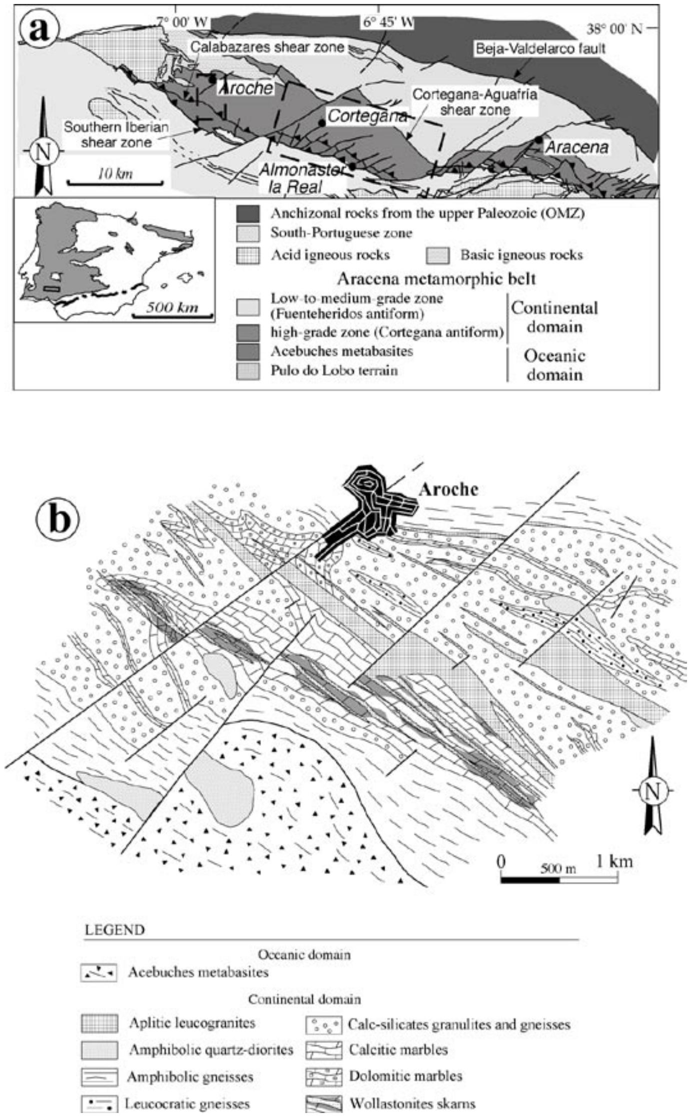

Fig. 1 (a and b).- a) The Aracena metamorphic belt (AMB) is located at the contact between the Ossa Morena and the South Portuguese zones of the Iberian Massif. Its trend (WNW-ESE) is parallel to the main structures of the Ossa-Morena Zone. The insets show detailed geological maps of the two areas considered in the present study. b) A small area of the contact between the oceanic and the continental domains (OD and CD, respectively) located to the south of Aroche.

Fig. 1 (a y b).- a) La banda metamórfica de Aracena (AMB) se localiza en el contacto entre las zonas de Ossa Morena y Sudportuguesa del Macizo Ibérico. Su orientación (ONO-ESE) es paralela a las estructuras principales de la Zona de Ossa Morena. Los recuadros corresponden a los mapas geológicos de detalle de las dos áreas consideradas en este estudio. b) Mapa de un sector del contacto entre los dominios oceánico y continental (OD y CD, respectivamente) localizada al sur de Aroche.

the CD). The structures in the CD do not affect the OD. In particular, the axial traces of the later folds are arranged in an *en-échelon* pattern, oblique with respect to the boundary with the amphibolites of the OD. The OD traverses the whole mapped area without any deflection related to those folds or older structures in the CD (Fig. 1b).

2.1. Acebuches metabasites of the OD

The Acebuches metabasites outcrop in a long (> 100 km), narrow (around 1 km wide) band with a WNW-ESE direction and dipping to the north. This band is disrupted by late variscan strike-slip faults, but shows a nearly constant thickness in the studied area (about 600 m). The Calabazares shear zone (Díaz Azpiroz, 2001 and figure 1a) separates the Acebuches metabasites from the CD of the AMB, located to the north. The metabasite sheet overlies to the south, through the Southern Iberian shear zone (SISZ, Crespo-Blanc and Orozco, 1988), the Pulo do Lobo terrain.

The main rock types of the Acebuches series are amphibolites with minor amounts of mafic schists and metadolerites. Detailed geochemical studies (Dupuy *et al.*, 1979; Munhá *et al.*, 1986; Quesada *et al.*, 1994; Castro *et al.*, 1996b) have shown that the parental rock of the Acebuches metabasites was an oceanic crust of MORB affinity. This crust was affected by a medium-to-high-grade metamorphic event that displays an inverted metamorphic gradient, with the highest temperature mineral assemblage located at the top of the series (to the north). Moreover, studies by Crespo-Blanc and Orozco (1988), Crespo-Blanc (1991), Castro *et al.* (1996b), Díaz Azpiroz and Fernández (2000; 2003) and Díaz Azpiroz (2001) have evidenced that after this first metamorphic stage, the SISZ imposed a retrograde metamorphism, related to the mylonitisation, that affected the lower half of the pile. Taking into account the effects that these two events produced in the Acebuches metabasites, four main rock types have been defined in this series (Díaz Azpiroz, 2001). These rock types are, from the structural top to the structural bottom: (1) banded amphibolites with clinopyroxene, (2) banded amphibolites without clinopyroxene, (3) sheared amphibolites and (4) mafic schists. The different facies appear in parallel bands that follow the structural pattern of the OD. These bands can be repeated by means of inverse shear zones related to the SISZ. Additionally, in those areas of the lower half of the pile preserved from deformation and metamorphism, metadolerites with a relict igneous fabric have been found.

The metabasites of the Acebuches series present plagioclase and hornblende as the principal phases (> 90 % of the modal composition). Nevertheless, modal differences have been found across the sheet. Three mineral assemblages have been defined in this series:

$$\mathrm{Pl + Hb \pm Qtz + Cpx + Ttn + Ilm + Mgt \pm Ap} \qquad (1)$$

$$\mathrm{Pl + Hb \pm Qtz + Ttn + Ilm + Mgt \pm Ap} \qquad (2)$$

$$\mathrm{Pl + Hb + Act + Ep \pm Qtz \pm Chl \pm Cal \pm Ttn \pm Ilm \pm Mgt} \qquad (3)$$

The first mineral assemblage is found in the banded amphibolites with clinopyroxene, which outcrop near the structural top of the metabasite pile, and it represents the highest metamorphic grade reached by the Acebuches series (Hb-Cpx zone). The mineral assemblage (2), corresponding to the Hb zone, appears in both the banded amphibolites without clinopyroxene and in the sheared amphibolites. These two rock types are located in the middle of the Acebuches series, between the banded amphibolites with clinopyroxene and the mafic schists. Finally, the mineral assemblage (3) is characteristic of the transition between the low-grade amphibolite and the greenschists metamorphic facies, and it corresponds to the mafic schists, which are located close to the structural base of the metabasite sheet. The mafic schists present, in the cores of porphyroblasts, plagioclases with oscillatory zoning as well as clinopyroxenes of augite composition. Both have been interpreted as relict phases which support the igneous origin of the Acebuches metabasites (Castro *et al.*, 1996b; Díaz Azpiroz, 2001).

The banded amphibolites appear in the upper half of the Acebuches series, and they show a characteristic centimetric to decimetric granulometric layering (Fig. 2a), which is parallel to a metamorphic foliation defined by the preferred orientation of amphibole prisms. The contacts are sharp and there are not significant differences in composition between bands (Castro *et al.*, 1996b). The banding is best developed near the top of the series, in the Hb-Cpx zone. On the contrary, the banded amphibolites of the Hb zone are medium-grained, lack the largest grain size bands and their banding is, therefore, less evident.

In the coarse-grained banded amphibolites leucosomes with subhedral to euhedral amphiboles as well as euhedral zoned plagioclases have been observed. This texture, along with a typical tonalitic mineral assemblage (Pl + Hb ± Cpx ± Qtz) suggests that these leucosomes could have been originated by partial melting of the amphibolite. Experimental melts obtained by dehydration melting of the Acebuches amphibolites are tonalitic in composition (López and Castro, 2001).

The lower half of the Acebuches series comprises sheared amphibolites and mafic schists. Both rock types

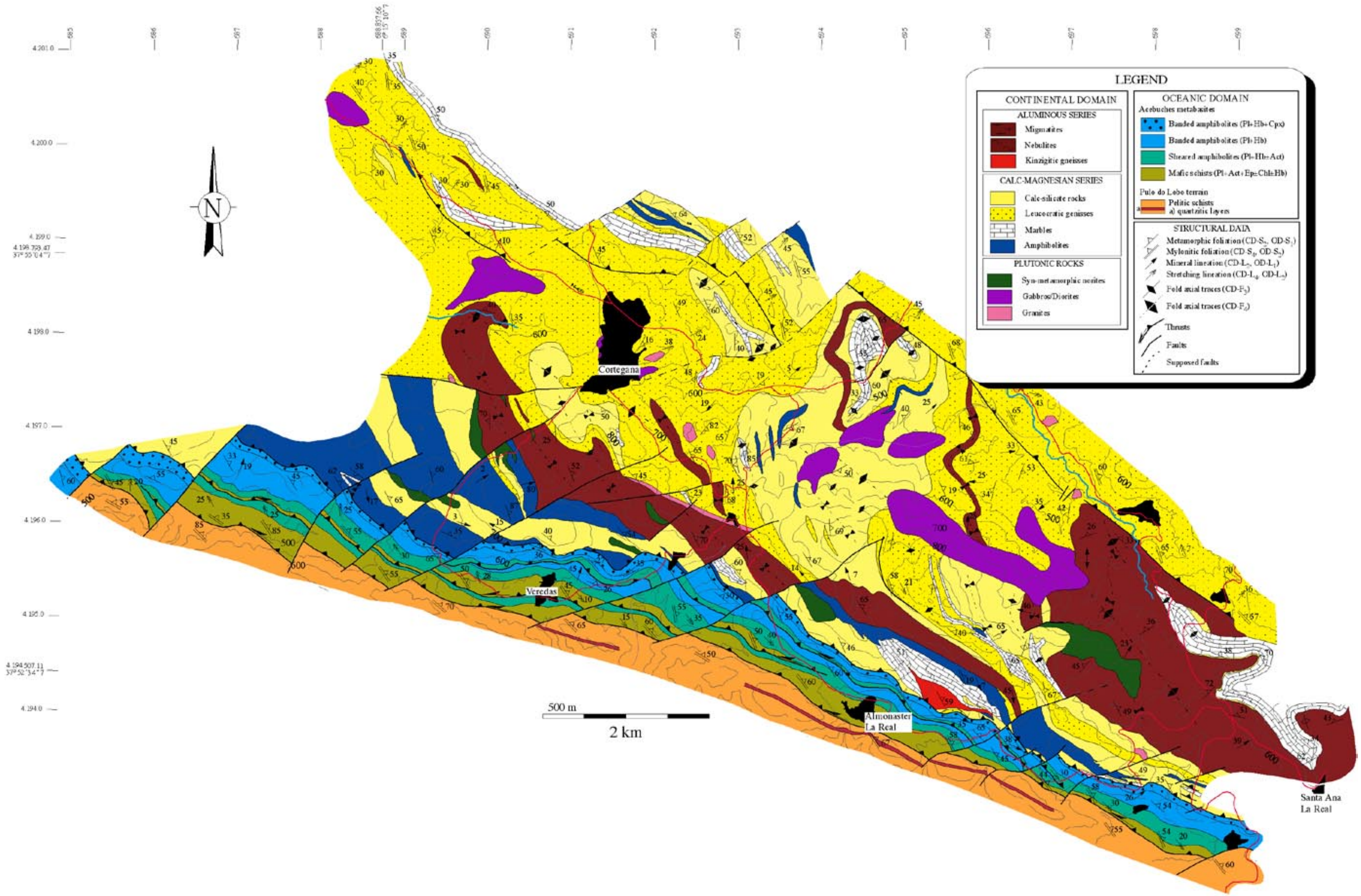

Fig. 1.- (cont) c) Map of the southern zone of the AMB between Cortegana and Santa Ana La Real (Díaz Azpiroz, 2001). The OD to the south and the CD to the north are clearly distinguished. Their structural features are very distinct. The OD shows several thrusts with an imbricate structure and with a constant trend (WNW-ESE). On the other hand, the structure of the CD is characterised by complex fold interference patterns, including fold traces with variable azimuths affected by a later folding event.

Fig. 1.- (cont) c) Mapa de la zona sur de la AMB entre Cortegana y Santa Ana La Real (Díaz Azpiroz, 2001). Se distinguen claramente el OD al sur y el CD al norte. Sus características estructurales son muy distintas. El OD muestra diversos cabalgamientos imbricados con una dirección constante (ONO-ESE). Por el otro lado, la estructura del CD se caracteriza por unos patrones de interferencia de pliegues muy complejos, incluyendo trazas de pliegues con direcciones variables que han sido afectados por un plegamiento posterior.

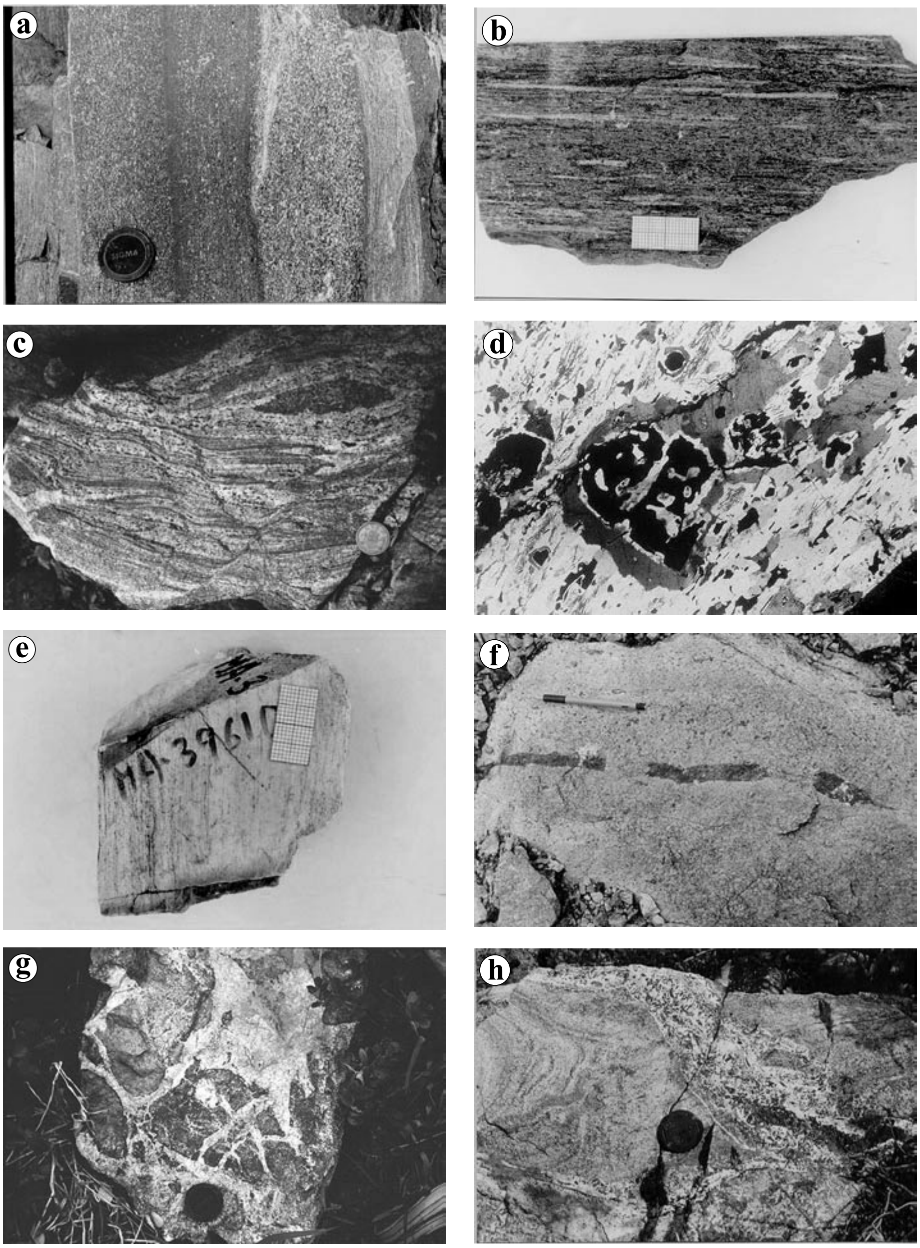

Fig. 2.- Photographs of different rock types found in the AMB. a) Coarse-grained banded amphibolites of the OD with alternating light coarse grained, grey medium grained and dark fine-grained bands. b) Mafic schists from the Acebuches metabasite series showing, on the mylonitic foliation planes, a penetrative stretching lineation. c) Stromatic migmatites of the CD, with a layering defined by alternating leucosome and melanosome layers. Also, paleosome bodies are observed at the top of the photograph. d) Kinzigitic gneisses of the CD. Skeletal blast of hercinite surrounded by a plagioclase rim. The matrix is constituted by dynamically recrystallised cordierite along with fibrolite aggregates. e) Leptinitic gneiss of the CD with a penetrative mylonitic foliation defined by pyroxene and amphibole blasts. f) Marbles of the CD. The metamorphic foliation is defined by melanocratic blasts (marked by the pen) as well as by the calc-silicate boudins. The tabular shape of the boudins suggests that the calc-silicate layers are much more competent than the surrounding marble. g) Calc-silicate rocks of the CD with agmatic texture. h) Pegmatitic Pl-Hb body showing intrusive relationships with foliated and folded calc-silicate rocks.

Fig. 2.- Fotografías de distintas litologías de la AMB. a) Anfibolitas bandeadas de grano grueso del OD, en la que alternan bandas claras de grano grueso, bandas grises de grano medio y bandas oscuras de grano fino. b) Esquistos máficos pertenecientes a las metabasitas de Acebuches mostrando, sobre los planos de foliación milonítica, una lineación de estiramiento penetrativa. c) Migmatitas estromáticas del CD, con un bandeado definido por una alternancia de capas de leucosoma y melanosoma. También se observan, en la parte alta de la fotografía, paleosomas. d) Gneises kinzigíticos del CD. Blasto esqueletal de hercinita rodeado por una corona de plagioclasa. La matriz está compuesta por cordierita recristalizada dinámicamente junto a agregados de fibrolita. e) Gneis leptinítico del CD con una foliación milonítica penetrativa definida por blastos de piroxeno y anfíbol. f) Mármoles del CD. La foliación metamórfica está definida por blastos de minerales melanocráticos (marcado por el bolígrafo), así como por *boudins* de rocas de silicatos cálcicos. La forma tabular de los *boudins* sugiere que las capas calcosilicatadas son mucho más competentes que el mármol que las rodea. g) Rocas de silicatos cálcicos del CD con una textura agmática. h) Cuerpo pegmatítico con Pl-Hb presentando relaciones intrusivas con rocas de silicatos cálcicos foliadas y plegadas.

are fine-grained and show a penetrative mylonitic foliation as well as a stretching lineation (Fig. 2b), which seem to be due to the deformation produced in the SISZ.

2.2. High-grade zone of the CD

To the north of the Acebuches metabasites is located the CD of the AMB which, according to its metamorphic grade has been divided into a high-grade zone, near the contact with the OD, and a low-grade zone to the north of the former (*e.g.*, Castro *et al.*, 1996a, b; 1999a). The high-grade zone coincides with the Cortegana antiform (see Bard, 1969; Giese *et al.*, 1994a). The southern overturned limb, dipping to the north, overthrusts the OD. The Cortegana-Aguafría shear zone (CASZ, Díaz Azpiroz, 2001) constitutes the northern boundary of the high-grade zone of the CD. The low-grade zone of the CD overthrusts the high-grade zone through the CASZ.

The subdivision proposed for the high-grade zone (Díaz Azpiroz, 2001) is based on (1) stratigraphic correlations with lower grade zones of the AMB (Bard, 1969; Crespo-Blanc, 1991; Giese *et al.*, 1994a), (2) compositional differences between lithologies and (3) field relationships. Two main rock series have been defined: the aluminous and the calc-magnesian series. According to Crespo-Blanc (1991), the aluminous series would correspond to the Precambrian La Umbría series, the marbles located at the base of the calc-magnesian series are correlated with the Cambrian Aracena dolomitic series and, finally, the calc-magnesian series would coincide with the bimodal volcano-sedimentary formation.

Aluminous series

The aluminous series is composed mainly of high-grade metapelitic gneisses, with subordinate intercalations of graphite rich quartzites, calc-silicate rocks and marbles. These rocks were partially molten giving rise to migmatites. According to different proportions of partial melt, stromatic migmatites (Fig. 2c), agmatic migmatites and nebulites have been defined. The contacts between different types of migmatites, although not always appear clearly, seem transitional (Castro *et al.*, 1999a; Díaz Azpiroz *et al.*, 2002). Díaz Azpiroz *et al.* (2002) have described stromatic and agmatic migmatites whereas nebulites are well studied in El-Biad (2000).

The main mineral assemblage of the aluminous migmatites is:

$$\mathrm{Qtz + Pl + Bt + Kfs \pm Crd \pm Grt \pm Sil \pm Ms \pm Opx \pm Sp \pm Amp \pm Cpx \pm Ap \pm Opaques.} \quad (4)$$

Differences in composition of the original protolith, as well as in the partial melting reactions gave rise to different rock types, which have been defined in base of the minor phases present in melanosomes (El-Biad, 2000; Díaz Azpiroz, 2001). In this sense, biotitic (± Sil), cordieritic (Crd ± Grt ± Sil), amphibolitic (Amp ± Cpx ± Crd) and charnockitic (Crd + Opx ± Sil) migmatites have been defined. Throughout the series, leucosomes can be granitic (*s.s.*), trondhjemitic or tonalitic in modal composition.

In stromatic and agmatic migmatites, foliation is defined by alternative milimetric layers of leuco- and melanosomes (Fig. 2c). This migmatitic layering is parallel to the regional foliation and is pervasively folded at the outcrop scale. In some stromatic migmatites, the limits between leuco- and melanosome layers are diffuse, suggesting a continuous variation in the melt fraction between bands. Frequently, leucosomes appear in veins injected through a set of fractures crosscutting all the previous structures but connected with the concordant leucosome layers. Migmatitic layering embraces enclaves of quartzites, amphibolites or calc-silicate rocks.

Leucosomes can be isotropic or, alternatively, they can present a weak foliation defined by the preferred orientation of isolated blasts and biotitic aggregates defining a schlieren fabric. In all cases, a relict sequential igneous texture is observed in leucosomes, comprising subhedral feldspars, euhedral zoned plagioclases and undeformed quartz grains.

The aluminous series also includes kinzigitic gneisses appearing in decametre-scale bodies located near the contact between the CD and the OD. These gneisses have been studied by El-Biad (2000) and Díaz Azpiroz (2001). Its mineral assemblage is:

$$\mathrm{Crd \pm Grt \pm Kfs \pm Hc + Sil \pm Pl \pm Ilm \pm Bt \pm Qtz} \quad (5)$$

Cordierite appears either as subhedral megacrysts with crenulated fibrolite aggregates in the core or as dynamically recrystallised blasts (Fig. 2d). Hercynite crystals show a skeletal habit and are associated with fibrolite and rims of plagioclase. The kinzigitic gneisses present a rough and irregular compositional layering, defined by dark cordierite-rich layers and light layers with K-feldspar and almandine-rich garnet. The mineral assemblage, with prevalence of dehydrated phases, together with the observed fabric, suggests a probable restitic origin for these rocks (El-Biad, 2000; Díaz Azpiroz, 2001).

Calc-magnesian series

The calc-magnesian series comprises different rock types such as leucocratic gneisses, calc-silicates rocks, amphibolites and marbles, whose common protolith could have been a bi-modal volcano-sedimentary series of upper Cambrian-middle Ordovician age (Bard, 1969; Apalategui *et al.*, 1983; 1984; Crespo-Blanc, 1991).

a) Leucocratic gneisses

Leucocratic gneisses are mainly composed of quartz and feldspar and both quartz-feldspatic and trondhjemitic have been found. The main mineral assemblage is:

$$Qtz + Pl \pm Kfs \pm Bt \pm Amp \pm Cpx \pm Grt \pm Gr \pm Ep \pm Chl \pm Ms \pm Ttn \pm opaques \pm Tur \pm Ap \pm Zrn \pm Mnz \pm Aln \quad (6)$$

According to the predominant minor phase, biotitic, amphibolic, pyroxenic and, to a lesser extent, garnet-rich and graphitic leucocratic gneisses have been defined (Díaz Azpiroz, 2001). Alternating layers formed by different types of leucocratic gneisses and, also, lateral transitions between them are common.

The above mentioned compositional layering is parallel to a metamorphic foliation defined by trails of the ferro-magnesian minerals. Usually, a mineral lineation defined by the preferred orientation of amphibole and clinopyroxene is observed on the foliation planes. When deformed at shear zones, a very penetrative mylonitic foliation, which embraces numerous feldspar porphyroclasts, and an associated stretching lineation are observed (Fig. 2e).

b) Calc-silicate rocks and marbles

In the high-grade zone of the CD, a suite of calc-silicate rocks and marbles occurs as discontinuous bands and lenticular bodies, and appears spatially associated with leucocratic gneisses, amphibolites, quartzites and graphitic gneisses.

The marbles can either outcrop as hectometric, pervasively folded sheets located at the base of the calc-magnesian series or intercalated within the calc-silicate rocks. In both cases, marbles are characterised by coarse-to-medium-grained granoblastic textures. Based on the carbonated phases present, impure calcitic and dolomitic marbles have been distinguished:

$$Cal + Di + Phl \pm Qtz \pm Wo \quad (7)$$

$$Dol + Fo\ (+Srp) + Phl \pm Spl \pm Pl \pm Di \pm Amp \pm Ttn \quad (8)$$

The main foliation of these marbles comprises both a compositional layering and a metamorphic foliation defined by trails of ferro-magnesian minerals, which were rigidly rotated during deformation (Chacón Muñoz *et al.*, 2001). Additionally, calc-silicate and amphibolite bands, which have been interpreted as intercalated volcanic layers in the primitive carbonate series (Crespo-Blanc, 1991; Díaz Azpiroz, 2001), appear parallel to the main foliation of the dolomitic marbles (Fig. 2f). Most of these basic intercalated layers appear boudinaged (Fig. 2f). Although these boudins vary greatly in shape and size (up to 1 m wide), they usually show nearly rectangular sections with occasional development of fish-mouth limits. Chocolate-tablet structures have been observed as well (Díaz Azpiroz and Fernández, 2001).

Calc-silicate rocks comprises a wide variety of rock types, with strong differences in both textural relations and mineral composition, that reflect the effects of a HT/LP metamorphic event that affected a wide range of sediments and volcanic rocks with a variable proportion of carbonates. The most common mineral assemblage corresponds to calc-silicate granulites and calc-silicate gneisses:

$$Pl + Cpx \pm Amp \pm Opx \pm Qtz \pm Grt \pm Ep \pm Ol \pm Ttn \pm Cal \pm Kfs \pm Wo \pm Scp \pm opaques \pm Sp \pm Ap \quad (9)$$

Additionally, magnesian and calcic skarns and skarnoids are included in this suite of rocks.

c) Amphibolites

The continental amphibolites that outcrop in the high-grade zone appear usually related to calc-silicate rocks, near the contact with the OD. Occasionally, the main structures of marbles and calc-silicate rocks appear crosscut by fine-grained amphibolitic dikes. The continental amphibolites show important variations in grain size along with a consistent mineral assemblage:

$$Pl + Hb \pm Cpx \quad (10)$$

The most characteristic continental amphibolites of the high-grade zone are coarse and very coarse-grained amphibolites (defined as El Rellano amphibolites by Castro *et al.*, 1996b), which appear intercalated within calc-silicate rocks and marbles. These amphibolites are isotropic rocks that were not affected by the main deformation event of the CD, and they crosscut previous structures of surrounding calc-silicate rocks (Fig. 2h).

The fine-grained amphibolites usually show a well-developed granoblastic texture, although subhedral zoned plagioclases suggest an igneous origin for these rocks. On the other hand, the El Rellano amphibolites can either present a typically metamorphic granoblastic or a dominant igneous texture.

Intrusive rocks

Basic intrusions parallel to the main structures of the high-grade zone of the CD have been reported (Bard, 1969; Castro *et al.*, 1996a, b; El-Hmidi, 2000). Ambiguous relationships between the intrusions and their host rocks have been interpreted by El-Hmidi (2000) as an evidence of the syn-metamorphic character of these intrusions.

The basic syn-metamorphic intrusive rocks are characterised by the assemblage

$$Cpx + Opx + Pl + Qtz \pm Ilm \pm Mgt \quad (10)$$

with biotite and hornblende as retrograde phases developed after ortopyroxene. Three main magmatic facies (accumulated norites, non-accumulated norites and dioritoids) can be distinguished. The cartographic distribution of these facies suggests that the Los Molares pluton might represent a magmatic chamber, with the more basic accumulated facies at the base and the more differentiated facies at the roof.

The accumulated norites are characterised by an igneous layering defined by millimetre-scale bands of orto- and clinopyroxene as cumulus phases, with plagioclase as the main intercumulus phase.

Apart from the mentioned metanoritic syn-metamorphic plutons, post-kinematic intrusions are also observed in the high-grade zone of the CD (Díaz Azpiroz, 2001; Díaz Azpiroz *et al.*, 2001). Intermediate-to-basic intrusions comprise gabbros, diorites, quartz-diorites, and subordinate tonalites and norites. On the other hand, small plutons of meta-aluminous leucocratic granites have been described by Díaz Azpiroz *et al.* (2001).

3. Structure

The main structures in the AMB are E-W to WNW-ESE oriented and dip to the north (Fig. 1a). The northern boundary of the AMB is the Beja-Valdelarco fault, which separates the AMB from the rest of the OMZ. The contact between the CD and the OD is outlined by a thrust vergent to the south, the Calabazares shear zone. The Southern Iberian shear zone (SISZ), first defined by Crespo-Blanc and Orozco (1988) marks the southern boundary of the OD metabasites. The SISZ is considered as the limit between the OMZ and the SPZ. Kinematically, the SISZ shows a strike-slip sinistral movement, with a component of top-to-the-south thrust. To the south of the SISZ is located the Pulo do Lobo terrain, interpreted by Eden (1991) as an accretionary prism. Although the Pulo do Lobo is traditionally considered as a part of the SPZ (*e.g.*, Bard, 1969; Schermerhorn, 1971), its tectonic evolution is more akin to that of the metabasites of the OD (the Acebuches metabasites). Therefore it is here included as a part of the OD (Castro *et al.*, 1996a, b, Díaz Azpiroz, 2001). The Santa Bárbara thrust marks the southern boundary of the Pulo do Lobo terrain.

The structural characteristics of the AMB have been studied by, among others, Apalategui *et al.* (1983; 1984; 1990); Barranco *et al.* (1983); Crespo-Blanc and Orozco (1988; 1991); Abalos *et al.* (1991); Fonseca and Ribeiro (1993) and Giese *et al.* (1994a, b). One of the most remarkable geological features of the AMB is the striking difference between the OD and CD in their structural configuration and tectonic evolution (Fig. 1b) (Castro *et al.*, 1996a; Díaz Azpiroz *et al.*, 1999; 2003b; Díaz Azpiroz, 2001). The description of the structures is accordingly separated into two different sections devoted to the study of the OD and the CD, respectively.

3.1. Oceanic domain

In this work the description is focused in the structure of the Acebuches metabasites, which is a key to the deciphering of the tectonic evolution of the contact between the ZOM and the ZSP. The Acebuches metabasites constitute a band of more than 100 km in length and with a thickness of less than 1 km (Figs. 1a, c), and dipping consistently between 40° and 50° towards north. Three deformation phases have been identified in the metabasites of the OD (Castro *et al.*, 1996b). The OD-D_1 is associated with a high-grade metamorphic stage, and affected the entire metabasite sheet. A strong deformation gradient is observed, with an increase in the deformation value towards the top of the metabasite pile (Díaz Azpiroz, 2001, Díaz Azpiroz and Fernández, 2003), in parallel with the increase in the recorded metamorphic temperatures (Castro *et al.*, 1996b). The main fabric developed during this phase is a foliation defined by the preferred orientation of amphibole and plagioclase crystals (OD-S_1). Other structures include a lineation (OD-L_1) marked by the alignment of amphibole crystals and an extensional crenulation cleavage (C' planes, Ponce de León and Choukroune, 1980) defining an anastomosing pattern. The OD-S_1 is best developed at the top of the amphibolite sheet where it is parallel to a prominent banding in the amphibolites. This banding has been interpreted by Castro *et al.* (1996a) as a result of the high-grade metamorphism of the upper part of the amphibolitic pile. Also, the OD-S_1 foliation is sub-parallel to the boundaries of the amphibolite sheet (Fig. 3a). The kinematic criteria appearing in the upper part of the amphibolites indicate the activity of a predominantly non-coaxial deformation history for OD-D_1. These criteria include S-C composite planar fabrics (Berthé *et al.*, 1979), asymmetric porphyroblast systems (*e.g.*, Passchier and Trouw, 1996) and C' planes. Considering the high pitch shown by the OD-L_1 (Fig. 3a), the kinematic criteria consistently indicate a top-to-the south sense of movement, with a minor component of sinistral strike-slip movement.

The second deformation phase (OD-D_2) corresponds to the activity of the Southern Iberian shear zone. Coeval to the movement along the SISZ is a retromorphism of the amphibolites towards greenschist facies. The SISZ mainly affected the lower half of the amphibolite sheet and the upper part of the Pulo do Lobo metasediments. However,

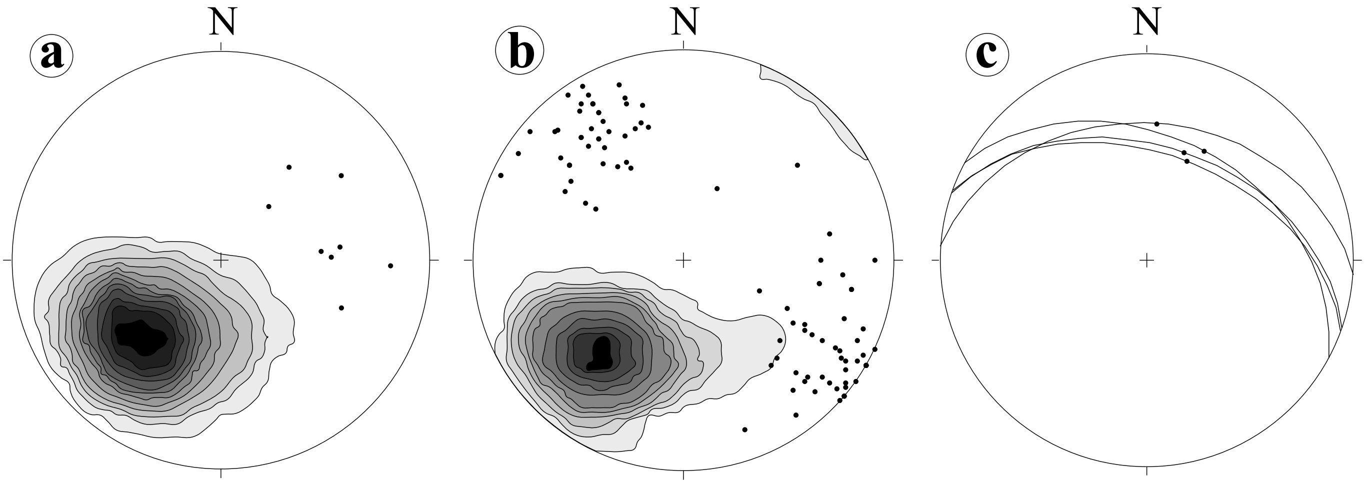

Fig. 3.- Lower-hemisphere, equal-area, projections of foliation and lineation data from the Acebuches metabasite series. Kamb contour and contour intervals are 2σ. **a**) OD-S_1 (98 poles to planes) and OD-L_1 (8 lines). **b**) OD-S_2 (205 poles to planes) and OD-L_2 (98 lines). **c**) OD-S_3 (4 planes) and OD-L_3 (4 lines).

Fig. 3.- Proyecciones equiareales (hemisferio inferior) de datos de foliación y lineación de las metabasitas de Acebuches. Diagramas de densidad de polos con intervalo de contornos de 2σ. **a**) OD-S_1 (98 polos de planos) y OD-L_2 (8 líneas). **b**) OD-S_2 (205 polos de planos) y OD-L_1 (98 líneas). **c**) OD-S_3 (4 planos) y OD-L_3 (4 líneas).

its geometry is quite intricate in detail, with many minor shear zones kinematically linked to the floor shear zone, defining an imbricate fan (Fig. 1c). A prominent S-L fabric was formed in association with the activity of the SISZ. OD-S_2 is mylonitic and it is marked by the preferred orientation of amphibole prismatic blasts, plagioclase ribbons and millimetre-scale bands of epidote, actinolite and chlorite. Statistically, the orientation of the OD-S_2 is very similar to that of OD-S_1 (Fig. 3b). The OD-L_2 stretching lineation is defined by plagioclase ribbons and elongated amphibole blasts. OD-L_2 strikes NW-SE, with moderate plunges towards SE and NW (Fig. 3b). A fundamental fact is that OD-L_2 plunging towards SE are the more common in the amphibolite band, with opposite plunges dominating only in specific areas (Crespo-Blanc, 1991, Díaz Azpiroz, 2001). This spatial distribution of lineations with changing plunges is explained by Díaz Azpiroz (2001) as a consequence of the SISZ acting as a transpressive zone, according to the model of Lin *et al*. (1998). In this way, the areas with NW-plunging lineations are supposedly due to the influence of a more intense pure shearing component, when compared to the areas with SE-plunging lineations. Kinematic criteria help to decipher the shear sense for the simple shearing component in the SISZ. These include sheath folds, S-C composite planar fabrics, C' planes, asymmetric porphyroclast systems, and fragmented plagioclase crystals. They consistently indicate a sinistral strike-slip movement.

Finally, the OD-D_3 phase is limited to the effects of the Calabazares shear zone. The thickness of this band is of no more than 5 m, and affects the northern contact of the amphibolite sheet with the CD. Deformation within the Calabazares shear zone is highly heterogeneous, with the formation of a mylonitic foliation (OD-S_3) and a stretching lineation (OD-L_3) that also affect the rocks in the overlying continental domain. The spatial arrangement of these fabrics (Fig. 3c), and the kinematic criteria associated with them indicate a top-to-the-SSE sense of movement. This implies that the Calabazares shear zone can be considered as a thrust, and it is kinematically comparable with the structures resulting from the CD-D_4 phase of deformation in the continental domain.

3.2. Continental domain

The CD shows a very complex tectonic history (Bard, 1969; Apalategui *et al*., 1983; 1984; Crespo-Blanc, 1991; Giese *et al*., 1994a). The most relevant feature of the CD is the increase in the metamorphic grade from north to south (Figs. 1a, c). Díaz Azpiroz (2001) has completed a detailed structural study of the southern, high-grade region of the CD. According to this author, four different ductile deformation phases can be distinguished in the AMB. The structures resulting from the CD-D_1 phase are almost completely erased by the more recent phases, especially by CD-D_2. The CD-S_1 foliation is only preserved as polygonal arcs of mica blasts, scattered rootless folds and crenulated fibrolite crystals included in cordierite porphyroblasts. At a large scale, the CD-D_1 phase was associated with the formation of km-scale recumbent folds (Bard, 1969; Apalategui *et al*., 1983; 1984; Crespo-Blanc, 1991; Abalos *et al*., 1991; Giese *et al*., 1994a; Apraiz, 1998). The stratigraphic sequence in the high-grade zone of the AMB appears frequently inverted (Díaz Azpiroz, 2001). This can be best explained as a consequence of the presence of overturned limbs of CD-D_1 recumbent folds.

The fabric due to DC-D_2 is essentially planar (CD-S_2), with subordinated L-tectonites. In fact, the CD-L_2 lineation is only apparent along discrete, local shear zones that show a normal component of displacement. The analysis of the measured quartz *c*-axis fabrics (Díaz Azpiroz, 2001), with predominant small circle girdles normal to the CD-S_2, indicates that the strain ellipsoid was in the apparent flattening field, not far from the oblate ellipsoids line (*e.g.,* Schmid and Casey, 1986). The short axis of this ellipsoid was located in a vertical position. The coeval activity of discrete normal shear zones and flattening with a vertical shortening axis points to an extensional collapse or gravity spreading as the most probable tectonic regimes for CD-D_2. This deformation phase is contemporary with the high-grade metamorphic conditions in the southern part of the CD. The effects of the CD-D_1 and CD-D_2 phases are schematically shown in Figure 4a.

A third deformation phase (CD-D_3) originated symmetric upright folds (Figs. 1c, 4b). Typical wavelengths for the main CD-D_3 folds are of 1 to 2 km. A CD-S_3 rough foliation is only apparent in the hinges of minor folds in marbles. The axial traces of the CD-D_3 folds vary from the north of the CD, where they strike N-S, and are vertical, to the south of the CD, where they are WNW-ESE oriented, dipping towards the NNE (Fig. 1c). The superposition of the CD-D_3 folds with the overturned limbs of CD-D_1 gave place to the formation of antiformal synclines and synformal anticlines (Fig. 4b).

CD-D_4 is the last main phase affecting the CD. It is also the phase that contributed to a larger extent to the present map-scale structure of the CD. Two types of structures appear during this phase: large antiforms and ductile shear zones. Two antiforms essentially define the structure of the CD (Bard, 1969), the Fuenteheridos antiform to the north, and the Cortegana antiform to the south (Fig. 1c). Both show wavelengths of several km, and they are open folds moderately inclined towards the SSW. The superposition of these folds with those of the previous phases generated complex fold interference patterns (Díaz Azpiroz, 2001; Díaz Azpiroz et al., 2003b). To the south of the CD, dominate the type 0 interference pattern (Ramsay, 1967), that is, redundant superposition. To the north of the CD the 3-D relative disposition of the several generations of folds originated patterns corresponding to the types C, E, F, G and I of Thiessen and Means (1980). No tectonic fabrics were developed in association with these large folds. The boundary between the Cortegana and Fuenteheridos antiforms is outlined by a major WNW-ESE oriented shear zone, the Cortegana-Aguafría shear zone (Fig. 1a) (Crespo-Blanc, 1991, Díaz Azpiroz, 2001; Díaz Azpiroz et al., 2003b). A very penetrative mylonitic foliation (CD-S_4) appears within this shear zone, with an associated stretching lineation (CD-L_4). CD-S_4 dips 40°-45° to the north, and CD-L_4 shows a large pitch (Fig. 5). The kinematic criteria in this shear zone are scarce, but the quartz *c*-axis fabrics measured by Díaz Azpiroz (2001) unequivocally indicate a top-to-the-SSW sense of movement. This implies an almost pure thrust displacement for the Cortegana-Aguafría

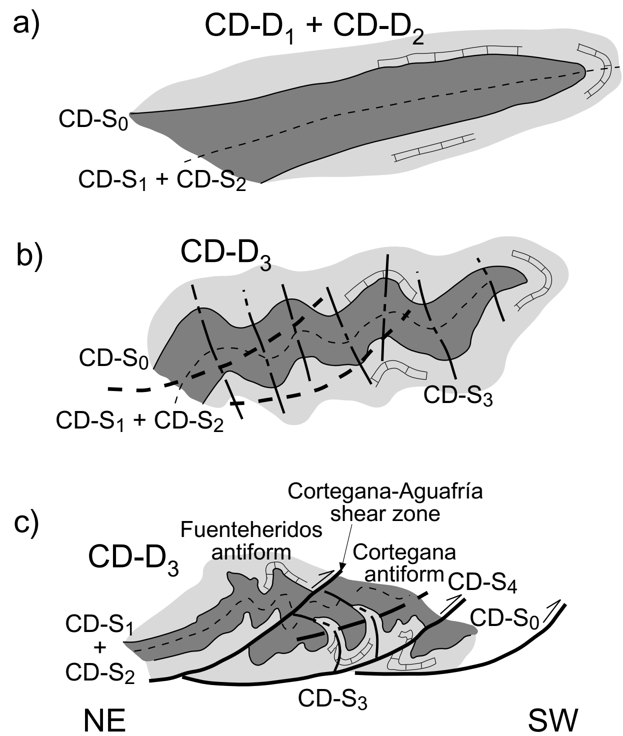

Fig. 4.- Schematic tectonic evolution proposed for the CD of the AMB (Diaz Azpiroz, 2001). a) As the result of the CD-D_1 and CD-D_2 deformation phases, km-scale recumbent folds and a high-temperature penetrative foliation (CD-S_2) were generated. b) CD-D_3 gave place to open symmetric upright folds. The discontinuous lines represent the localisation of the CD-D_4 shear zones. c) CD-D_4 produced km-scale thrusts, with a very penetrative mylonitic foliation (CD-S_4), and thrust accommodation folds (namely, the Fuenteheridos and the Cortegana antiforms).

Fig. 4.- Esquema del modelo de evolución tectónica propuesto para el CD de la AMB (Díaz Azpiroz, 2001). a) Como resultado de la acción conjunta de las fases CD-D_1 y CD-D_2 se formaron pliegues recumbentes de escala kilométrica y una foliación penetrativa de alta temperatura (CD-S_2). b) CD-D_3 dio lugar a pliegues verticales simétricos y abiertos. Las líneas discontinuas representan la localización de las zonas de cizalla de CD-D_4. c) CD-D_4 generó cabalgamientos de escala kilométrica con una foliación milonítica penetrativa (CD-S_4) y pliegues de propagación (los antiformes de Cortegana y Fuenteheridos).

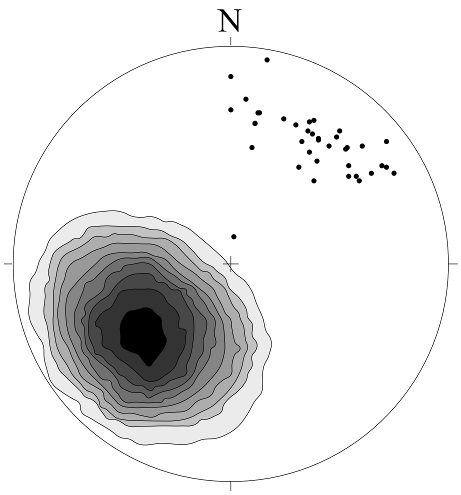

Fig. 5.- Lower-hemisphere, equal-area projection of poles to the CD-S_4 mylonitic foliation and the associated CD-L_4 stretching lineation (59 data). Kamb contours and contours are 2σ.

Fig. 5.- Proyecciones equiareales (hemisferio inferior) de polos de la foliación milonítica CD-S_4 (diagramas de densidad con intervalo de contornos de 2σ) y de la lineación de estiramiento CD-L_4 asociada (59 datos).

shear zone. Crespo-Blanc (1991), Giese *et al*. (1994a) and Díaz Azpiroz (2001) described similar structures, albeit of minor dimensions, in other parts of the CD. The Calabazares shear zone is kinematically comparable to these structures, and it might be considered as an equivalent of the Cortegana-Aguafría shear zone in the contact between the OD and the CD. Díaz Azpiroz (2001) envisages CD-D_4 as a phase of crustal shortening accommodated by the displacement of large blocks along ductile shear zones acting as a thrust system. The antiforms are accordingly interpreted as thrust nappes or, given the low strain in the antiforms evidenced by the generalised absence of CD-D_4 fabrics, as thrust accommodation folds (Fig. 4c).

4. Metamorphism

The AMB has been traditionally recognised as a high-temperature/low-pressure metamorphic belt (*e.g.*, Bard, 1969; Miyashiro, 1973; Grapes and Graham, 1978). Nevertheless, few studies dealing with the metamorphism of this area have been carried out, including those by Bard (1967a, b; 1969; 1970), as well as later works by Castro and co-workers (Castro *et al.*, 1996a, b; Díaz *et al.*, 1997; El-Biad *et al.*, 1997; El-Biad, 2000; Díaz Azpiroz, 2001). Based on these works, the present section deals with the metamorphic evolution of three different rock types of the AMB: the Acebuches metabasites of the OD and, on the other hand, the aluminous migmatites and the marbles of the CD.

4.1. Metamorphism of the Acebuches metabasites

Phase relations and metamorphic zones

The Acebuches metabasites underwent a HT/LP metamorphic event (OD-M_1) that gave place to an inverted gradient, taking into account the current position of the pile. Bard (1969) described a metamorphic zoning, based on the colours of amphiboles and calculated a very steep metamorphic gradient. On its turn, Crespo-Blanc and Orozco (1988) defined the Southern Iberian shear zone (SISZ), which depicts the southern limit of the Acebuches series. The deformation produced in the SISZ, that affected the lower half of the metabasite sheet, was accompanied by a retrograde metamorphic event in the greenschists facies (OD-M_2), which was most intense at the base of the pile. In consequence, the observed steep metamorphic gradient is the sum of two superposed events: a HT/LP event (OD-M_1) coeval to the OD-D_1 phase, with an inverted gradient, and a subsequent retrometamorphic event (OD-M_2) related to the SISZ (OD-D_2) that affected the lower half of the metabasitic pile.

The banded amphibolites from the upper part of the pile still preserve the metamorphic assemblages due to OD-M_1. The medium-grained banded amphibolites show a typical Hb zone mineral assemblage (Pl-Hb). Towards the top of the pile, the plagioclase becomes more calcic by means of the modal decrease of titanite (*e.g.*, Moody and Jenkins, 1983), until the trespassing of the Ttn-out isograde, which is evidenced by titanite included in ilmenite + magnetite grains (Díaz Azpiroz, 2001). The transition from the medium-grained to the coarse-grained amphibolites is marked by the Cpx-in isograde (Fig. 6). The appearance of clinopyroxene in the Acebuches amphibolites coincided with the partial melting of the rock, as evidenced by the presence of leucosomes with tonalitic composition. It seems likely that this process took place through the anhydrous melting reaction under low and medium pressures (P < 10 kbar) defined by López and Castro (2001):

$$\text{Hb} + \text{Pl} = \text{Cpx} + \text{melt} + \text{other minerals} \qquad \text{(R1)}$$

The metabasites from the lower half of the sheet show the assemblages formed during OD-M_2, which meant a retrograde metamorphic event. The sheared amphibolites show a characteristic Hb zone mineral assemblage, which is very similar to that of the medium-grained banded amphibolites. Therefore, it seems likely that in the medium part of the Acebuches series, the differences in P and T during the transition from OD-M_1 to OD-M_2 were not

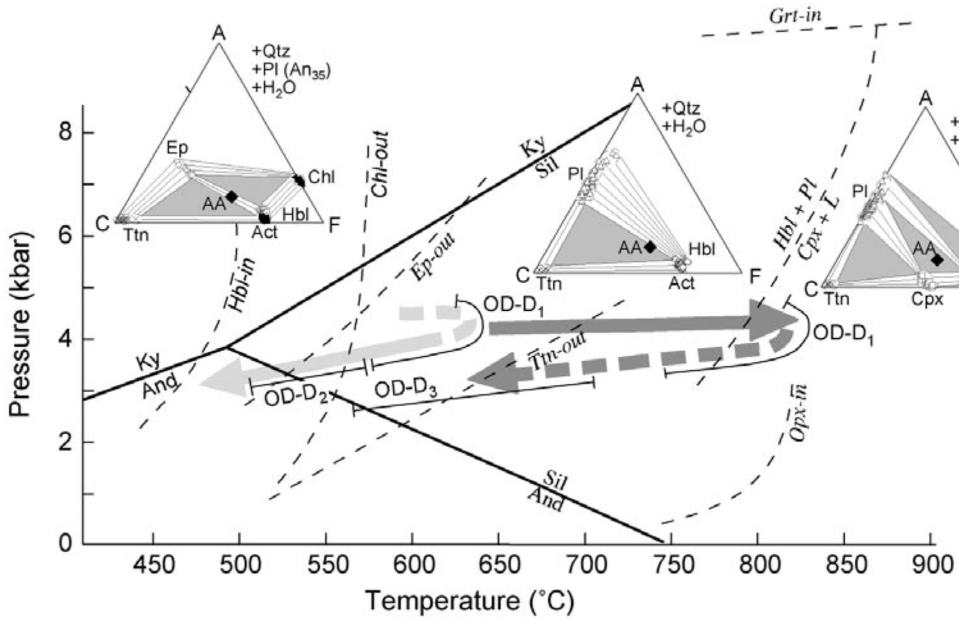

Fig. 6.- P-T-d paths deduced for the Acebuches metabasites: banded amphibolites with clinopyroxene (dark path) and mafic schists (light path). Solid lines correspond to paths deduced directly from observed mineral assemblages whereas dashed lines correspond to paths inferred by indirect observations. ACF diagrams showing the mineral assemblages corresponding to the three main metamorphic zones described across the Acebuches metabasite series. a) The upper levels of the sheet belong to the clinopyroxene zone. b) Most of the series are amphibolites with a typical Pl-Hb assemblage. c) The mafic schists from the lower levels display a Pl-Hb-Act-Ep-Chl mineral assemblage.

Fig. 6.- Trayectos P-T-d deducidos para las metabasitas de Acebuches: anfibolitas bandeadas con clinopiroxeno (trayectoria gris oscuro) y esquistos máficos (trayectoria gris claro). Las líneas sólidas corresponden a trayectorias deducidas directamente de las paragenesis minerales observadas, mientras que las líneas a trazos corresponden a trayectorias supuestas a partir de observaciones indirectas. Los diagramas ACF muestran las paragenesis minerales correspondientes a las tres zonas metamórficas descritas en la serie de Acebuches. a) Los niveles superiores de la lámina pertenecen a la zona del clinopiroxeno. b) La mayor parte de la serie son anfibolitas con una paragenesis típica con Pl-Hb. c) Los esquistos máficos de los niveles inferiores muestran una paragénesis con Pl-Hb-Act-Ep-Chl.

significant.

Near the base of the Acebuches metabasitic pile, the retrograde metamorphic event reached P-T conditions corresponding to the low amphibolites-greenschists facies transition (Fig. 6). This is evidenced by the presence of actinolite, epidote and chlorite, which are formed by means of the tschermakite molecule break down through reaction (Grapes and Graham, 1978; Spear, 1993):

$$\text{Ts} = \text{Act} + \text{Chl} + \text{Ep} + \text{Qtz} \qquad \text{(R2)}$$

as well as by the decreasing of the anorthite molecule content of the plagioclase through reaction (Grapes and Graham, 1978; Maruyama *et al.*, 1983):

$$\text{Ts} + \text{An} = \text{Chl} + \text{Ep} + \text{Qtz} \qquad \text{(R3)}$$

The absence of albite in the mafic schists is indicative of low-pressure metamorphism (*e.g.*, Hynes, 1982; Maruyama *et al.*, 1983). On the other hand, the coexistence of chlorite and epidote suggests that the pressure during OD-M_2 was around 4 kbar (see Díaz Azpiroz, 2001). Only at the base of the metabasitic sheet, the mineral assemblage approached the greenschists P-T conditions and albite is found, which was formed from edenite and quartz, through reaction (Grapes and Graham, 1978):

$$\text{Ed} + \text{Qtz} = \text{Act} + \text{Ab} \qquad \text{(R4)}$$

Mineral chemistry

Recently, mineral chemistry analysis on plagioclase and amphibole composition have been carried out by Castro *et al*. (1996b), Díaz *et al*. (1997) and Díaz Azpiroz (2001) to constraint the P-T conditions during metamorphism and to establish a detailed metamorphic gradient across the Acebuches metabasitic series.

The composition of plagioclase (more calcic near the top of the Acebuches series) is in agreement with the inverted position of the metamorphic gradient. Furthermore, the scarcity of albite in the mafic schists indicates the little significance of the peristerite *solvus* which, taking into account the medium temperatures reached by these rocks, is indicative of low-pressure conditions (see Maruyama *et al*., 1983; Laird, 1980; Laird and Albee, 1981).

The Acebuches metabasites present a very homogeneous whole-rock composition, their amphiboles crystallised under conditions of fO_2 around the QFM buffer and thus, variations in amphibole composition may be related to

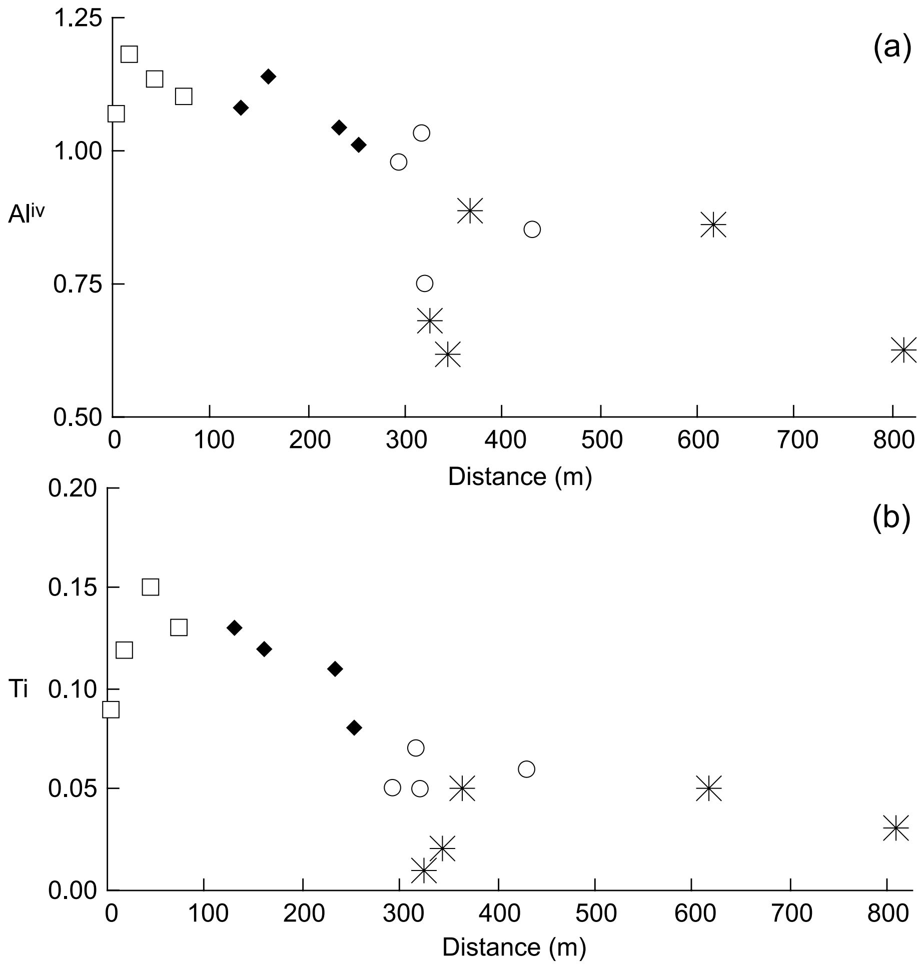

Fig. 7.- Evolution of the Al^{iv} (**a**) and Ti (**b**) in amphiboles from the Acebuches metabasites, with respect to the distance to the Calabazares shear zone (namely, the structural top of the series), in the Veredas cross-section (see figure 1b). Banded amphibolites with (open squares) and without (black rhombi) clinopyroxene, sheared amphibolites (open circles) and mafic schists (asterisks) are differentiated.

Fig. 7.- Evolución del Al^{iv} (**a**) y del Ti (**b**) en anfíboles de las metabasitas de Acebuches con respecto a la distancia a la zona de cizalla de Calabazares (el techo estructural de la serie), en el corte de Veredas (véase la figura 1c). Se pueden distinguir anfibolitas bandeadas con clinopiroxeno (cuadrados blancos), anfibolitas bandeadas sin clinopiroxeno (rombos negros), anfibolitas cizalladas (círculos blancos) y esquistos máficos (asteriscos).

changes in the P-T conditions (Castro *et al.*, 1996b).

A detailed analysis of Acebuches amphiboles (Castro *et al.*, 1996b; Díaz Azpiroz, 2001) show that, apart from the $FeMg_{-1}$ substitution, the compositional variability of these amphiboles took place through coupled substitutions that involve Al^{iv}, $(Na+K)^A$ and Ti, which are sensitive to temperature (*e.g.*, Grapes and Graham, 1978; Laird, 1980; Laird and Albee, 1981; Spear, 1981; Hynes, 1982; Blundy and Holland, 1990). On the other hand, substitutions with Na^{M4} involved, which are sensitive to pressure (Grapes and Graham, 1978; Laird and Albee, 1981), seem inactive. Therefore, compositional changes in Acebuches amphiboles are mainly due to temperature variations whereas pressure remained stable at low values.

According to this statement, analysis of the evolution in the amphibole composition through three cross-sections of the Acebuches series have been achieved (Castro *et al.*, 1996b; Díaz Azpiroz, 2001), in order to make an estimation of the metamorphic gradient within the metabasitic pile. Variations in Al^{iv} and Ti give the most valuable information (Fig. 7). In the banded amphibolites, the content of the mentioned elements decreases with the increasing distance to the top of the series, suggesting a temperature descent. This descent is also observed from temperature data (Díaz *et al.*, 1997; Díaz Azpiroz, 2001) obtained through the Hb-Pl thermometer (Holland and Blundy, 1994), and confirm the inverted position of the metamorphic gradient of OD-M$_1$. Unfortunately, the compositional variability observed in the sheared amphibolites and mafic schists do not allow establishing a similar variation of the metamorphic conditions during OD-M$_2$.

The relative importance of coupled substitutions in amphibole composition has been used by Castro *et al.* (1996b) to define a qualitative geothermobarometer, with a distorted P-T diagram appearance, which was applied to amphiboles from the Acebuches metabasites (Fig. 8). The amphiboles from the Acebuches series appear within the low-pressure area of the diagram and they arrange in a nearly horizontal path. Furthermore, the amphiboles from the coarse-grained Cpx-amphibolites project close to the Ed + Ts + (Ti-Ts) apex and, as the distance to the top of the series increases, amphiboles project closer to the Tr apex, pointing to a temperature descent. In summary, the path shows a nearly isobaric cooling from the top to the base of the Acebuches series.

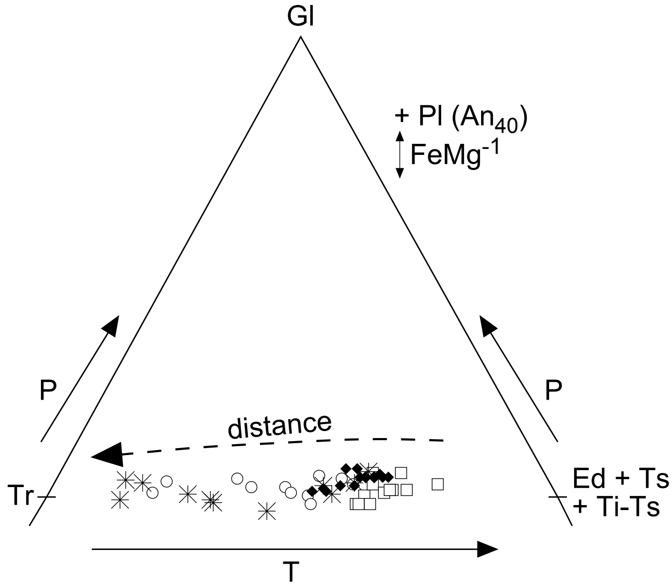

Fig. 8.- Qualitative thermobarometer (based on Castro *et al.*, 1996b) defined by a baricentric projection of amphiboles in the space Tr – Gl – Ed + Ts + Ti-Ts, through the $FeMg^{-1}$ interchange and from Pl (An_{40}). The curve marks the compositional evolution (with respect to the distance to the Calabazares shear zone) of the Acebuches amphiboles (symbols as in figure 7).

Fig. 8.- Termobarómetro cualitativo (basado en el propuesto por Castro *et al.*, 1996b) definido mediante una proyección baricéntrica de anfíboles en el espacio Tr – Gl – Ed + Ts + Ti-Ts, a través del intercambio $FeMg^{-1}$ desde Pl (An_{40}). La curva marca la evolución composicional (respecto a la distancia con la zona de cizalla de Calabazares) de los anfíboles de la serie de Acebuches (símbolos como en la figura 7).

4.2. Metamorphism of the aluminous series

Bard (1969) carried out a general study on the metamorphism of the CD of the AMB and determined that this region of the OMZ underwent a HT/LP metamorphic event. This statement is based on the absence of kyanite in the metapelites, as andalucite is found in the low-medium grade areas and sillimanite in the high-grade areas. In a recent study, El-Biad (2000) presented a detailed analysis of the HT/LP metamorphism that affected some of the lithologies comprised in the aluminous series: Los Molares migmatites and the Almonaster pelitic granulite (kinzigitic gneiss). This study was later completed by a brief report discussing the metamorphic evolution of the nebulites with charnockitic affinities (Díaz Azpiroz, 2001), which also belong to the aluminous series. A summary of the latter two is exposed.

Migmatites of the aluminous series

According to the petrographic study carried out by El-Biad (2000), the main mineral assemblage observed in the Los Molares migmatites reflects the divariant reaction

Bt + Sil + Qtz = Grt + Crd + Kfs + Melt (R5)

On the contrary, the mineral assemblage observed in the charnockitic migmatites suggests that ortopyroxene, instead of garnet, was formed during the dehydration melting of biotite through reaction

Qtz + Bt + Grt = Opx + Crd + Kfs + L (R6)

The distance between both migmatites is not long enough to presume significant pressure differences. Therefore, it seems more likely that the mentioned mineral variations are due to differences in composition (Bard, 1969; El-Biad, 2000; Diaz Azpiroz, 2001).

Relic grains of muscovite within K-feldspar poikiloblasts found in the Los Molares nebulites indicate that a previous partial melting event took place through reaction

Qtz + Ms = Or + Sil + Melt (R7)

On the other hand, the presence of spinel together with cordierite in the highest-grade areas suggests that some of these rocks surpassed the reaction

Grt + Sil = Sp + Crd + Qtz (R8)

The metamorphic path, as it has been deduced from the petrographic study, the deduced metamorphic reactions and the thermobarometric calculations, is shown in Figure 9. The retrograde paths corresponding to deformational phases CD-D_3 and CD-D_4 are simplified. Since these two phases are compressive the PT paths should show a pressure increment. Nevertheless, mineral assemblages and metamorphic reactions defined in the high-grade rocks of the CD do not reflect such pressure ascent. It is remarkable that two dehydration partial melting reaction have contributed to the generation of melts in this area. The complete dehydration of the muscovite through reaction R7 and the onset of biotite dehydration through reactions

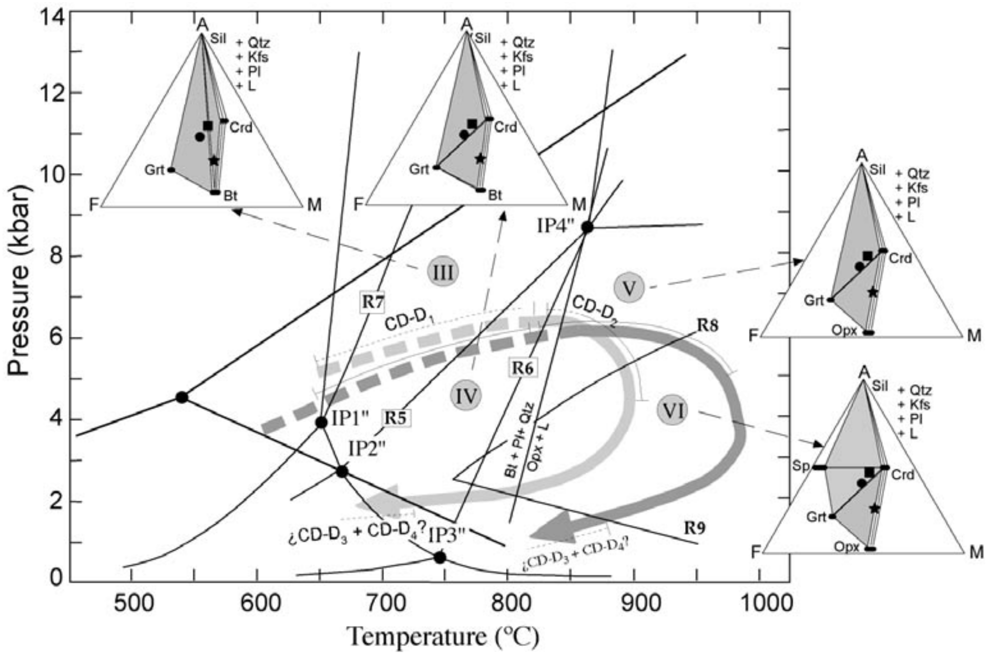

Fig. 9.- P-T-d paths deduced from petrography for Los Romeros migmatites, Los Molares nebulites and the charnockitic nebulites (light path), as well as for the kinzigitic gneisses (dark path) of the aluminous series of the CD (El-Biad, 2000; Díaz Azpiroz, 2001). Solid segments were deduced directly from observed textures, whereas dashed segments were inferred from indirect observations. Roman numbers indicate stability fields crossed by the deduced paths, which are characterised by their respective mineral assemblage represented in AFM diagrams. The black circle stands for the Los Romeros migmatites and the Los Molares nebulites whole rock composition (El-Biad, 2000). The black square stands for the kinzigitic gneiss whole rock composition (El-Biad, 2000) and the black star stands for the theoretical composition of the charnockitic nebulites.

Fig. 9.- Trayectos P-T-d, deducidos a partir del estudio petrográfico, de las migmatitas de Los Romeros, las nebulitas de Los Molares y las nebulitas de afinidad charnockítica (trayectoria gris claro), así como de los gneises kinzigíticos (trayectoria gris oscuro), de la serie alumínica del CD (El-Biad, 2000; Díaz Azpiroz, 2001). Los segmentos sólidos corresponden a trayectorias deducidas directamente de las texturas observadas, mientras que los segmentos a trazos corresponden a trayectorias supuestas a partir de observaciones indirectas. Los números romanos indican los campos de estabilidad cruzados por las trayectorias deducidas, y se encuentran caracterizados mediante sus paragenesis respectivas, representadas en los diagramas AFM. El círculo negro representa la composición de roca total de las migmatitas de Los Romeros y las nebulitas de Los Molares (El-Biad, 2000). El cuadrado negro representa la composición de roca total de los gneises kinzigíticos (El-Biad, 2000) y la estrella negra representa la composición teórica de las nebulitas de afinidad charnockítica.

R5 and R6 suggest that temperature reached, at least, 825 ºC. On the other hand, reactions R5 and R6 did not occurred completely since there is biotite present in the CD metapelites. Therefore, the temperature did not reach the Bt-out isograde, which corresponds to 920-975 ºC, depending on pressure (Patiño Douce and Johnston, 1991). The deduced heating path could have been either isobaric or accompanied by a slight pressure increase. Anyway, pressure should have been low during the whole process, as it is deduced by the absence of kyanite (Bard, 1969). El-Biad (2000) carried out P-T calculations using Grt-Crd and Grt-Bt pairs (Perchuk and Lavrent'eva, 1983; Perchuk, 1991), GABIP and GABIT geothermometers (Patiño Douce and Johnston, 1991) and the Crd-Grt-Sil-Qtz geobarometer (Perchuk and Lavrent'eva, 1983). The results arisen from this study confirm the P-T path deduced from the petrographic analysis. In this sense, the nebulites reached higher temperatures (slightly over 900 ºC) than the stromatic migmatites (temperatures below 900 ºC). The obtained pressure values fluctuate from 4 to 6 kbar and depict a nearly isobaric path.

Kinzigitic gneisses

As it was previously indicated, the kinzigitic gneisses show a compositional layering, defined by alternating dark hercinite-rich and light garnet-rich bands. The dark bands are characterised by simplectites formed of anorthite-rich plagioclase and skeletal hercinite surrounded by fibrolite-free cordierite aureoles, whereas cordierite from the matrix shows relict fibrolite inclusions (see figure 2d). These simplectites are interpreted as the result of the complete consumption of garnet (Patiño Douce *et al.*, 1997), through the decompression reaction R8.

In the light bands, garnet shows reabsorbed rims and hercinite is very scarce. It seems likely that in this case, reaction R8 took place as well, but consumed the available sillimanite, which only appears as relict inclusions within cordierite.

According to this interpretation, the layering is due to compositional differences in the original schist, which would presents quartz-rich and mica-rich bands formed probably by metamorphic differentiation during folding. Both layers underwent the same two consecutive partial melting events (namely, muscovite dehydration melting and biotite dehydration melting). In the quartz-rich layers, sillimanite (a product of the muscovite dehydration melting) would have been consumed giving place to the light garnet-rich layers, whereas in the mica-rich layers reaction R8 would have consumed garnet generating the dark hercinite-rich layers. In both cases, the scarcity of quartz suggests that the produced melts were segregated from the system (El-Biad, 2000).

During the cooling path of these rocks, hercinite from the light layers was consumed through reaction

$$\text{Hc} + \text{Qtz} = \text{Fe-Crd} \qquad \text{(R9)}$$

which could not take place in the dark layers since there was not enough quartz present to react with hercinite. This is the reason why light layers are hercinite-poor whereas dark layers are hercinite-rich.

The metamorphic evolution of the kinzigitic gneisses is shown in figure 9. The temperature reached by these rocks was over 920 ºC (higher than that reached by the Los Molares migmatites), as it is deduced by the absence of biotite (El-Biad, 2000). Thermobarometric calculations have been carried out by Patiño Douce *et al*. (1997) and El-Biad (2000), using both the TWEEQU multiequilibrium geothermobarometer (Berman, 1991) and the Bt-Ilm geothermometer. These studies show that (1) the thermal evolution of the garnet growth is consistent with a prograde metamorphic event, (2) the peak temperature reached by these rocks (950-1000 ºC) represent the peak temperature of the CD and (3) the pressure of the metamorphism was between 5 and 6 kbar.

4.3. Metamorphism of the marbles from the calc-magnesian series

A suite of granulite-facies marbles and calc-silicate rocks occur as discontinuous bands and lenticular bodies throughout the continental domain of the AMB. Many of the marbles in the Aroche sector of the AMB (see figure 1c) were intruded by granitoids overprinting contact metamorphism effects after the peak of the regional metamorphic event. In the contact aureoles, calc-silicate rocks with

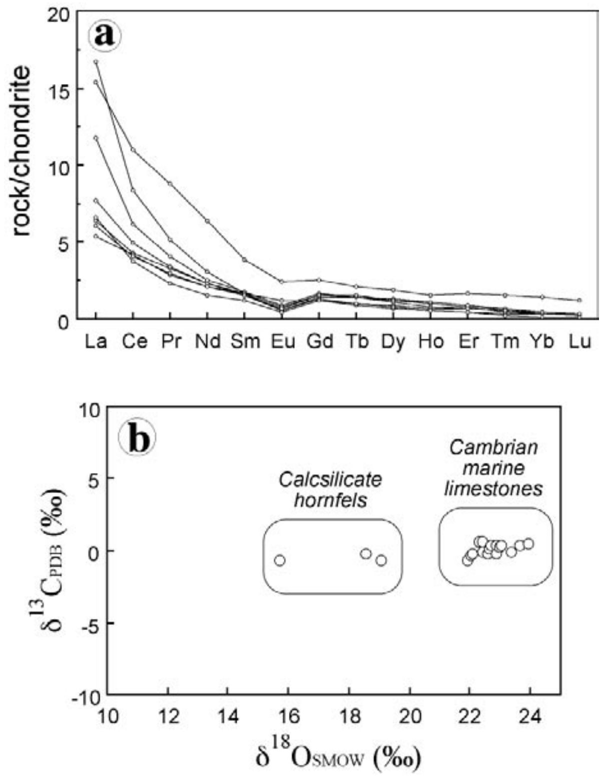

Fig. 10.- REE patterns (a) and isotopic ratios (b) of representative calcitic marbles from the Aroche sector.

Fig. 10.- Patrones de REE (a) y razones isotópicas (b) de mármoles calcíticos representativos del sector de Aroche.

diverse mineral assemblages were formed by metasomatic interaction between marble and magmatic-derived fluids taking place extensive calcic and magnesian skarns (Fernández-Caliani *et al*., 2001).

In general, the marbles are composed of various mineral assemblages whose phase equilibria can be constrained in terms of the system CaO – MgO – SiO_2 – Al_2O_3 + (H_2O-CO_2) fluid. On the basis of the dominant mineralogy, two contrasting metamorphosed carbonate rocks (namely, calcitic and dolomitic marbles) have been identified. Metamorphic effects were different depending on the carbonate rock composition.

Transformation of limestone into calcitic marble was determined by a simple textural readjustment with negligible mineralogical changes because the number of phases derived from impure limestone is clearly limited. A compositional banding parallel to the foliation is defined by modal variations of diopside and phlogopite. The massive calcitic marbles usually contain scattered quartz crystals that still remain unaffected at high-grade metamorphism. Mineral equilibria considerations and geochemical signature suggest that the calcitic marbles formed a closed or nearly closed-system apparently equilibrated with an internally derived and compositionally buffered fluid phase. In fact, the marbles show similar REE patterns (Fig. 10a) which reflect that the light REE are enriched over the heavy REE (La_N/Yb_N= 10.6-52.2), together with a slight negative Eu anomaly (Eu_N/Eu^*_N= 0.35-0.85). Negligible mobility of REE during metamorphism is evident from the similarity of all observed REE patterns in marbles. The isotopic composition (Fig. 10b) reveals that the marbles preserve their original sedimentary signatures in spite of intense metamorphic recrystallisation. The observed lower values of $\delta^{18}O$ are in the typical range of calc-silicate hornfels (Bowman, 1998). Nevertheless, formation of wollastonite through the reaction

$$CaCO_3 + SiO_2 = CaSiO_3 + CO_2 \qquad (R10)$$

occurred locally during prograde metamorphism under external influences. The occurrence of wollastonite in association with quartz segregations implies local interaction of water-rich fluids with marbles because this phase is stable under granulite facies only at low CO_2 fugacity (Valley, 1985). In this regional metamorphic scenario, the reactive fluids could be derived from water released by prograde dehydration of the surrounding rocks. Therefore, the massive calcitic marbles acted as barriers to fluid flow during metamorphism although they were locally permeable along the pre-metamorphic fracture system. Effects of channelized fluid infiltration are much more evident at the contact-metamorphic aureoles in the Aroche sector, where extensive wollastonite-skarn deposits were formed in a complex hydrothermal system that constitutes a spectacular example of fluid-rock interaction (Fernández-Caliani *et al.*, 2002; Moreno-Ventas *et al.*, 2002).

On the other hand, the peak metamorphic mineral assemblage of the dolomitic marbles includes elongated crystals of forsterite disseminated within a matrix of massive dolomite with minor calcite. Some of the dolomitic marbles also contain flakes of phlogopite and subhedral grains of green spinel. In some places, the dolomitic marbles contain intercalated calcsilicate bands, most of which appear to have been boudinaged. These bands display well-defined mineralogical zones consisting of diopside, locally replaced by tremolite, and a reaction rim formed by millimetre-scale concentric alternating bands of calcite and forsterite with minor phlogopite. Occasionally, quartz appears as a relict phase within the central diopsidic core. Formation of this skarnoid is related to the CD-D_2 deformation phase resulting in extension and boudinage of the calc-silicate bands, and it is closely followed by the development of bimetasomatic diffusion under chemical potential gradients. All stages of growth of the reaction rims are present. The first metamorphic reaction

$$Dol + 2Qtz = Di + 2CO_2 \qquad (R11)$$

led to the formation of diopside between the dolomite matrix and the quartz boudins in equilibrium with an internally buffered virtually pure CO_2 fluid. At more advanced stages of metamorphism, diopside became an unstable phase after a short time buffering process, resulting in formation of the forsterite-calcite outer rim by reaction.

$$3Dol + Di = 4Cal + 2Fo + 2CO_2 \qquad (R12)$$

Subsequent infiltration of water-rich fluids during retrograde metamorphism resulted in the replacement of diopside by tremolite and forsterite by serpentine.

5. Geochemistry and igneous petrogenesis

5.1. Oceanic metabasites

The first geochemical studies carried out by Bard (1969), Dupuy *et al*. (1979), Munhá *et al*. (1986) and Quesada *et al*. (1994) demonstrated the oceanic provenance of the Acebuches metabasites. In a more recent work, Castro *et al*. (1996b) accomplished a more accurate analysis to constraint the magmatic source and the later metamorphic evolution of these rocks.

According to the work by Castro *et al*. (1996b), the Hb-Pl amphibolites show major element patterns typical of tholeiitic basalts. Moreover, the low contents of immobile incompatible elements as well as the REE and ε_{Nd} data are characteristic of oceanic tholeiites (MORB). The MORB-normalised spidergrams (Pearce, 1983) of the Hb-Pl amphibolites show patterns similar to that of N-MORB for some immobile elements, but are enriched in Th and Nb (Fig. 11), which lie between N-MORB and P-MORB patterns (Saunders, 1984), suggesting that these amphibolites derived from transitional-type MORBs. The REE patterns are characteristic of transitional tholeiites (T-MORB) and, on a Ce_n/Yb_n vs Yb_n diagram, most of the normal Acebuches amphibolites plot in the field of T-MORB (Castro *et al*., 1996b).

To determine the source nature of the Acebuches metabasites, representative paired samples of Hb-Pl amphibolites and quartz-rich amphibolites, which appear in alternative layers, were selected for major and minor element and Sm-Nd isotope analyses (Castro *et al*., 1996b). For every pair, the Nd isotope ratio of the quartz-rich amphibolites is lower than that of the respective Hb-Pl amphibolite and tie lines linking every pair are parallel to one another. The quartz-rich amphibolites are enriched in the major oxides, trace elements and REE with respect to the normal amphibolites, but both rock types show parallel but separate trends for most of the major oxides and trace elements (Fig. 12). Moreover, the tie lines linking quartz-rich amphibolite and Hb-Pl amphibolite pairs are parallel. These features suggest the occurrence of a multiple fractionation process. According to Castro *et al*. (1996b), this implies the existence of a multi-chamber system beneath the ridge. In this scenario, every magma chamber, starting from similar compositions, underwent similar fractionation processes to separated closed systems.

The Acebuches amphibolites show a wide range in the $\delta^{18}O$ value (3.7-8.8 ‰). Furthermore, the increase in $\delta^{18}O$ is accompanied by an increase in mobile incompatible elements. These features may reflect a process of hydrothermal alteration during seawater interaction (Castro *et al*., 1996b), which can only affect the upper 2-3 km of the oceanic crust (McCulloch *et al*., 1980; Gregory and Taylor, 1981). These data clearly support the oceanic origin of the Acebuches metabasites, and suggest that they could come from the metamorphism and later exhumation of the uppermost part of an oceanic crust.

5.2. Syn-metamorphic noritic intrusions and related rocks

A detailed study devoted to the Los Molares basic syn-metamorphic intrusion has been carried out by El-Hmidi (2000). As it was previously mentioned, three magmatic facies can be distinguished in this pluton. The modal variability observed among these three facies (decreasing of pyroxene and increasing of plagioclase and hydrated Fe-Mg phases from the more basic rocks to the dioritoids) is consistent with a magmatic differentiation process involving fractionated crystallisation and crystal accumulation. The

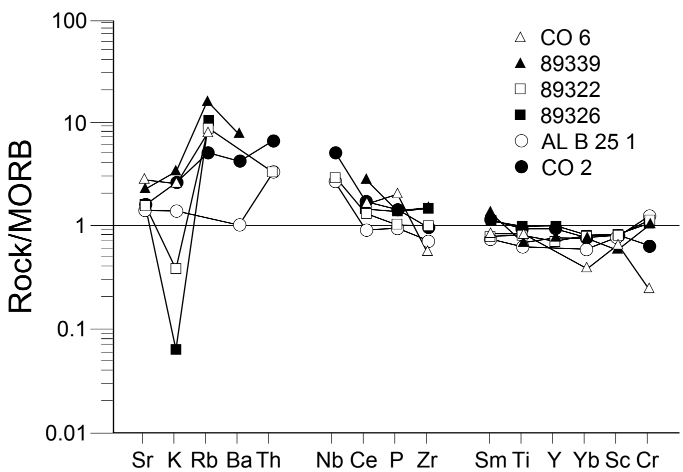

Fig. 11.- Rock/MORB normalised spider-diagrams with representative samples of the Acebuches metabasites (from Castro *et al*., 1996b).

Fig. 11.- Diagramas araña normalizados Roca/MORB con muestras representativas de las metabasitas de Acebuches (de Castro *et al*., 1996b).

petrographic study shows that both ortho- and clinopyroxene are early phases and, in the accumulated norites, constitute the essential cumulus phases. Moreover, the chemical variations shown by the main mineral phases can be interpreted in terms of magmatic differentiation processes or, otherwise, in terms of post-magmatic changes. Finally, the major elements variations observed in pyroxenes are consistent with changes in magma composition during its fractionation.

The major chemical analyses show a linear correlation between Al_2O_3, Na_2O and MgO, due to plagioclase fractionation. At the same time, the linear correlation between FeO, MnO and MgO suggests that both ortho- and clinopyroxene are the main ferro-magnesian phases that fractionated during the differentiation processes. The dioritoids are enriched in SiO_2 and Al_2O_3 and depleted in MgO, FeO and CaO with respect to the more basic facies. This chemical pattern might be the result of a fractional crystallisation process, which mainly involved pyroxene and plagioclase. On the other hand, the observed variations in the refractory element (Ti, Cr, Sc, Co and V) contents are consistent with the fractionation of ferro-magnesian phases like ortho- and clinopyroxene and hornblende, and also with the accumulation of the pyroxenes. Moreover, Eu anomaly is negative in the accumulated facies and slightly positive in the other two facies. This fact shows again the importance of plagioclase fractionation in the noritic rocks of the AMB. In consequence, the major element geochemistry, the REE diagram and the refractory elements contents of the Los Molares intrusive rocks suggest that the non-accumulated norites could represent the original magma, from which the dioritoids were differentiated by means of the fractional crystallisation of the accumulated norites through the accumulation of pyroxenes and plagioclase.

The non-accumulated norites are characterised by high MgO (7.21-11.01 %), SiO_2 (52-58 %), Cr and LREE contents together with low TiO_2 (0.36-0.66 %), P_2O_5 (0.01-0.14 %), HFS elements and HREE contents. This chemical features are similar to that of the high-Mg andesites (i.e., boninites), which have been related to atypical subduction zones (*e.g*., Meijer, 1980; Crawford *et al*., 1981; 1989; Cameron *et al*., 1983). Furthermore, in the MnO-TiO_2-P_2O_5 triangular discrimination diagram (Mullen, 1983), most of the basic rocks from the Los Molares intrusion plot in the calcic boninites field (Fig. 13), near Ca-rich boninites from different localities. In consequence, El-Hmidi (2000) interpreted the non-accumulated norites from the Los Molares intrusion as the plutonic equivalent of the calcic boninites.

The basic rocks from the Los Molares intrusion show $\delta^{18}O$ values between 8 and 10 ‰, which are higher than those corresponding to the mantle (Rollinson, 1993).

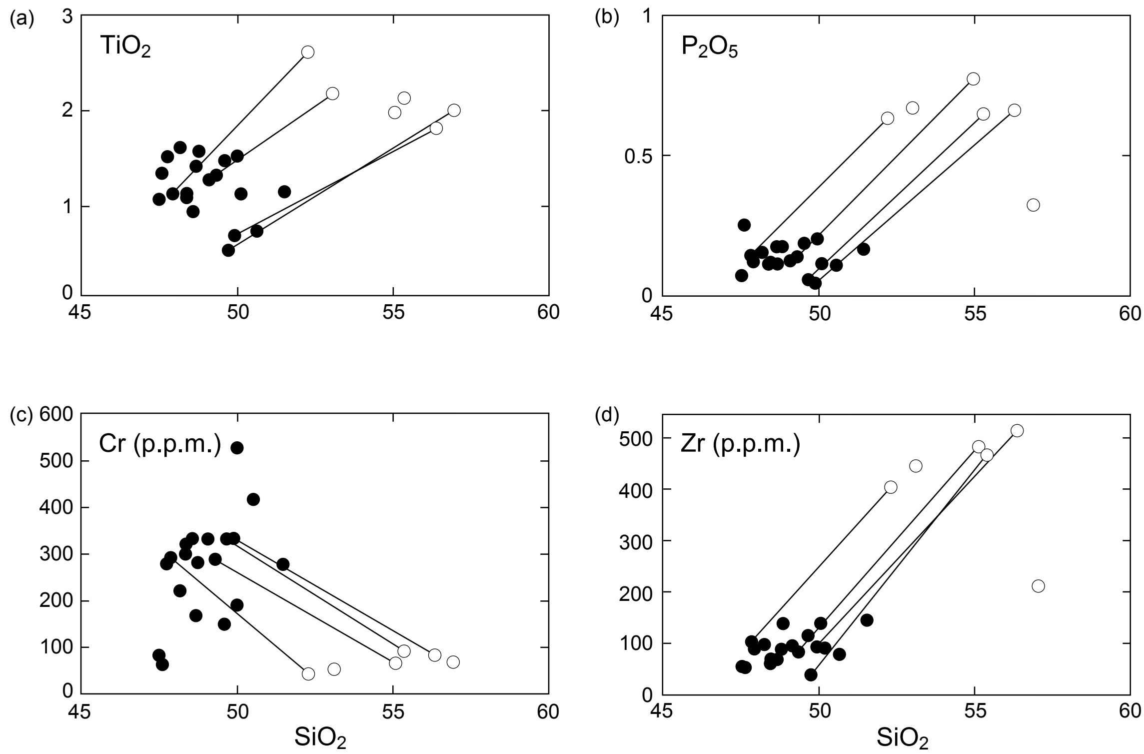

Fig. 12.- Silica variation plots for major and trace elements, showing the relationships between Pl-Hb and quartz-rich amphibolites from the Acebuches series. Tie-lines link pairs of samples from two adjacent layers (from Castro *et al*., 1996b).

Fig. 12.- Diagramas de variación de elementos mayores y trazas respecto a la sílice, mostrando las relaciones entre anfibolitas con Pl-Hb y cuarzoanfibolitas de la serie de Acebuches. Las líneas de coexistencia unen pares de muestras obtenidos de bandas adyacentes (de Castro *et al.,* 1996b).

Therefore, these rocks may have originated from an enriched source or, alternatively, from a depleted source that was previously metasomatised (Castro *et al*., 1996b; El-Hmidi, 2000). Moreover, the initial epsilon values are negative for Nd ($\varepsilon_{Nd340} < 0$) and positive for Sr ($\varepsilon_{Sr340} > 0$) for the three analysed samples, indicating an enriched source. On the contrary, the major element and trace element geochemistry (high Mg # and high Cr and Ni contents) suggests a depleted source. The presence of an enriched component in boninites generation has been proposed by several authors (*e.g*., Cameron *et al*., 1983; McCulloch and Cameron, 1983; Nelson *et al*., 1984; Crawford *et al*., 1989). El-Hmidi (2000) interprets these features as the result of the interaction between a refractory source (the mantle wedge) and an enriched component that could come from metasomatic fluids and partial melts derived from the subducting oceanic slab, from the oceanic subducted sediments or from the combination of both elements. Although different tectonic models have been proposed to explain boninite petrogenesis (*e.g*., Meijer, 1980; Crawford *et al*., 1981; Hickey and Frey, 1982; Rogers *et al*., 1989), all of them seem to be related to an atypical subduction context. This is because in normal subduction zones, the hydrated column generated beneath the fore-arc never reaches the hydrated peridotite solidus curve (>> 1000 ºC, Kushiro *et al*., 1968) and, therefore, no magmatism occurs in this zone. Instead, under anomalous high thermal gradient conditions, the hydrated peridotite may undergo a partial-melting event that produces boninitic magmatism. Different authors (Meijer, 1980; Crawford *et al*., 1981; 1989; Rogers *et al*., 1989; Tatsumi and Maruyama, 1989) have related this high thermal gradient to the presence of an oceanic spreading ridge close to the subduction zone.

5.3. Late meta-aluminous granites

Little attention has been paid to the late intrusive rocks that appear in the CD of the AMB. A recent work by Díaz Azpiroz *et al*. (2001) deals with some geochemical characteristics of a group of small plutons of meta-aluminous leucogranites.

The meta-aluminous character of these granites, shown by different geochemical diagrams, is consistent with the absence of mica and the presence of amphibole, clinopyroxene, garnet and titanite as minor phases. In a ORG normalised spidergram (Pearce *et al*., 1984), the late granites of the CD show a pattern similar to that of the granites related to continental collision tectonic scenario. Moreover, in the R1-R2 diagram (La Roche *et al*., 1980) with the fields added by Batchelor and Bowden (1985), the meta-aluminous granites of the CD of the AMB plot in the late-orogenic granites field. These observations are in agreement with the late intrusion of these small granitic plutons during the last stages of the continental collision that gave rise to the AMB (Díaz Azpiroz *et al*., 2001).

6. Isotope geochronology

The main features of the AMB and the time relationships between them, which are exposed elsewhere in this paper, led Castro *et al*. (1996a, b) to propose a tectonic model for this belt. The knowledge of the ages of some of those features is crucial in contrasting the proposed model. In this sense, absolute age determinations were presented in two recently published papers (Castro *et al*., 1999a; Díaz Azpiroz *et al*., 2002). Furthermore, a previous work by Dallmeyer *et al*. (1993) has also contributed with valuable Ar-Ar age data.

Rb-Sr isochrons in stromatic migmatites, nebulites and metanorites, Sm-Nd isochrons in metanorites and Ar-Ar dating of hornblende separates from amphibolites were calculated in the mentioned papers.

The results of these geochronological studies support that all the thermal events of the AMB took place during the Variscan orogeny, in a 30 Ma period during Early Carboniferous (Visean to Namurian). However, appreciable differences have been found along and across the metamorphic belt. The Ar-Ar dating of the amphibolites from the OD (Dallmeyer *et al*., 1993; Castro *et al*., 1999a) has shown an age evolution along the belt (Fig. 14). This is interpreted as the age of the HT/LP metamorphic event that affected these rocks (OD-M_1). This age evolution is consistent with the migration of the thermal focus along the belt towards the east, at a rate of around 0.5 cm a^{-1}. On the other hand, differences in age have been reported across the belt, in such a way that the ages calculated in the CD through layer-sampling technique (see Castro *et al*., 1999a; Díaz Azpiroz *et al*., 2002), are older than the ages for the oceanic amphibolites located in the same traverse. That is, there is an age pattern in the CD parallel to the observed pattern of the OD (Fig. 14). This observation suggests that the metamorphism of the continental hanging wall occurred earlier than that of the oceanic sheet located in the corresponding traverse.

On the other hand, Dallmeyer *et al*. (1993) presented $^{40}Ar/^{39}Ar$ mineral ages for the Beja gabbro, which intruded the AMB in the Portuguese sector. The obtained data (339.5 ± 1.0 Ma and 337.9 ± 1.0 Ma) are interpreted as cooling ages, and have not been proved to be crystallisation ages.

7. Experimental petrology

The hypothesis concerning the petrogenesis of some relevant lithological types in the AMB have been tested by experimentation in high-pressure piston-cylinder apparatuses. This section contains the main results of this approach, including a discussion of the melting conditions of the Acebuches amphibolites (López and Castro, 2001) and of the aluminous gneisses (El-Biad, 2000), as well as the generation of the syn-metamorphic basic magmatism (El-Hmidi, 2000).

Experiments were carried out in an end-loaded, solid-medium piston-cylinder apparatus at the University of

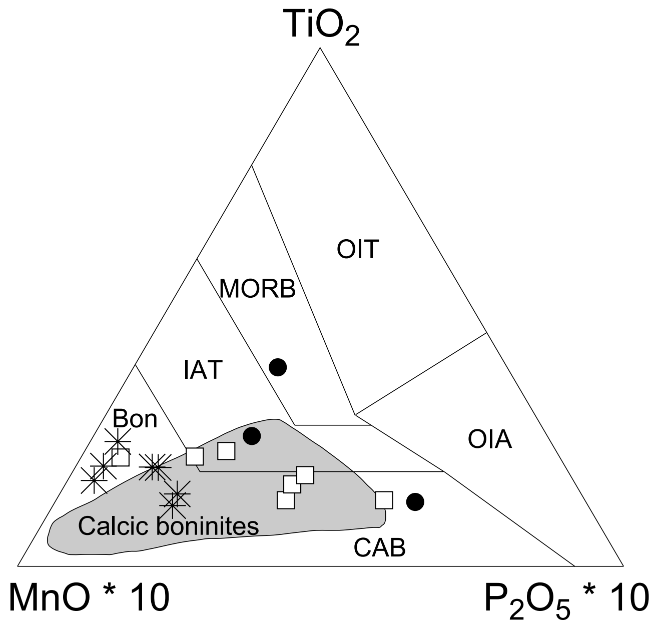

Fig. 13.- Representation of cumulated norites (asterisks), non-cumulated norites (squares) and dioritoids (circles) from the AMB (El-Hmidi, 2000) in the triangular TiO_2–MnO * 10–P_2O_5 * 10 diagram (Mullen, 1983). Fields are MORB (Mid Ocean Ridge Basalt), OIT (Ocean Island Tholeiite), OIA (Ocean Arc Alkali basalt), CAB (island-arc Calc-Alkaline Basalt), IAT (Island-Arc Tholeiite) and Bon (Boninite). The shaded area encloses representative analyses of calcic boninites from the Troodos complex in Cyprus (Rogers *et al*., 1989), the Tonga trench in the Pacific Ocean (Falloon *et al*., 1989) and the Vestfold Hills in the Antarctic shield (Kuhener, 1986).

Fig. 13.- Representación de noritas acumuladas (asteriscos), noritas no acumuladas (cuadrados) y dioritoides (círculos) de la AMB (El-Hmidi, 2000) en el diagrama triangular TiO_2–MnO * 10–P_2O_5 * 10 (Mullen, 1983). Los campos mostrados son: MORB (basalto de dorsal oceánica), OIT (toleíta de isla oceánica), OIA (basalto alcalino de arco oceánico), CAB (basalto calco-alcalino de arco de islas), IAT (toleíta de arco de islas) y Bon (boninitas). El área sombreada incluye análisis representativos de boninitas cálcicas procedentes del complejo de Troodos, en Chipre (Rogers *et al*., 1989); de la fosa de Tonga, en el Océano Pacífico (Falloon *et al*., 1989) y de las colinas de Vestfold, en el escudo antártico (Kuhener, 1986).

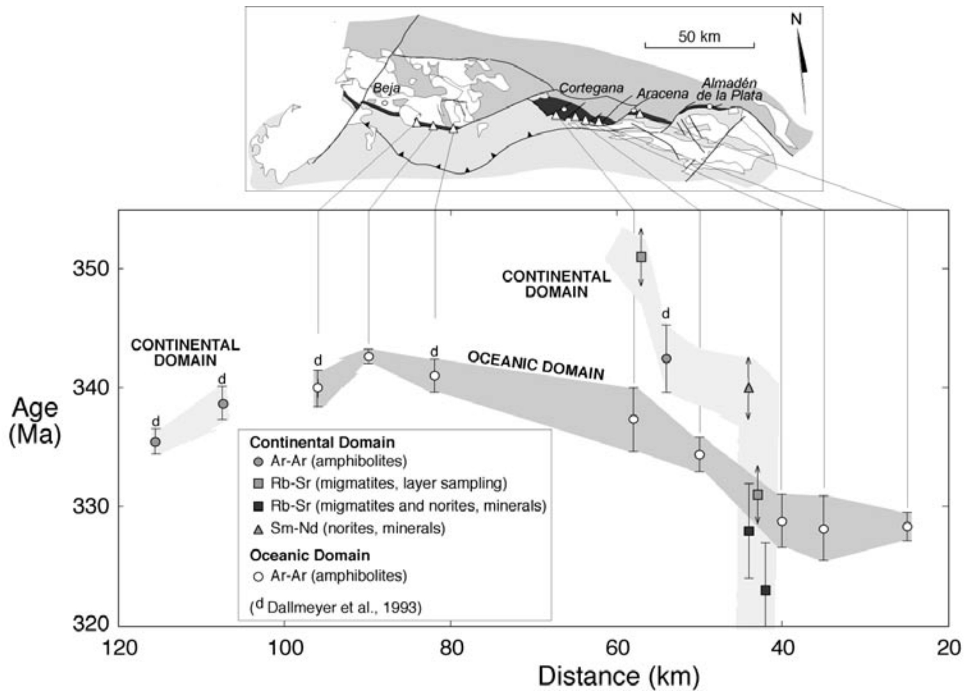

Fig. 14.- Variation of age of metamorphism with distance along the Acebuches metabasites, discarding the effect of displacements by late faults. The origin is arbitrarily located in Almadén de la Plata. Ages obtained in the rocks of the CD are also shown. The arrows are indicative of larger error bars (from Castro *et al*., 1999a).

Fig. 14.- Variación de la edad del metamorfismo con la distancia a lo largo de las metabasitas de Acebuches, descartando el efecto del desplazamiento producido por fallas tardías. El origen se localiza de manera arbitraria in Almadén de la Plata. También se muestran las edades obtenidas en rocas del CD. Las flechas son indicativas de barras de error mayores (de Castro *et al*., 1999a).

Huelva, with 12.7 mm (0.5 inch) diameter NaCl-graphite or CaF2-graphite cell assemblies. Samples were contained in welded Au capsules (graphite-Pt for high temperatures), 2.4 mm inner diameter with 0.3 mm wall. The capsules contained 10 mg of dry sample and, in the experiments with added water, this was added with a micro-syringe. Oil pressures were measured with electronic DRUCK PTX 1400 pressure transmitters, connected to OMRON E5CK controllers. Temperatures were measured and controlled with Pt_{100}–$Pt_{87}Rh_{13}$ thermocouples wired to Eurotherm 808 controllers (see Castro *et al*., 1999b for details).

7.1. Dehydration melting of the Acebuches amphibolites

The starting material used in the experiments was a MORB-derived amphibolite from the OD of the AMB. Its mineral assemblage consists of hornblende (49 vol. %), plagioclase (An_{44}) (46 vol. %) and ilmenite (5 vol. %). The experiments were carried out at temperatures between 750 and 950ºC and pressures of 4, 6, 10, 12 and 14 kbar. According to the experimental results, the melting reaction is peritectic and it involves formation of clinopyroxene, ortopyroxene, garnet or epidote and a tonalitic melt (López and Castro, 2001). For pressure conditions below 10 kbar the dehydration melting produced clinopyroxene as well as melt. On the other hand, for pressures higher than 10 kbar, epidote was produced at temperatures near the solidus, whereas garnet was the stable peritectic phase at temperatures higher than 850 ºC. Melt composition was tonalitic for all the studied P-T conditions. However, slight compositional changes with variations in the experimental conditions were observed. In this sense, Ti, Fe, Mg and Ca contents increased with pressure. Therefore, leucotonalitic compositions were obtained for the higher considered pressures.

The partial melting of amphibolites is a process triggered by high geothermal gradients (Martin, 1999). The PT path determined in the OD of the AMB (Díaz Azpiroz, 2001) crosscuts the fluid-absent solidus curve of the Acebuches amphibolites (López and Castro, 2001). In fact, leucocratic veins (<1 vol. %) can be observed at the top of the Acebuches amphibolites, where clinopyroxene is also present (Castro *et al*., 1996b). Therefore, it can be concluded that the top of the Acebuches amphibolitic sheet underwent a partial melting process coeval to the peak of the OD-M_1 metamorphic phase.

7.2. Melting of the aluminous gneisses

The aluminous gneisses have been used as starting material in melting experiments by El-Biad (2000). The goal of these experiments was the understanding of the melting processes governing the generation of migmatites and nebulites in the CD of the AMB. The starting material was tonalitic in composition, with a mineral assemblage composed of biotite, plagioclase, quartz, K-feldspar, graphite and oxides. The experiments without added water were carried out under pressure conditions between 3 and 10 kbar and temperatures ranging from 850 to 980 ºC. In the experiments with added water, the pressure conditions varied between 2 and 10 kbar, with temperatures between 650 and 750 ºC. The water-absent melting runs produced a granitic melt, whereas the hydrated melting runs gave place to a granodioritic melt. Comparison of the petrologic characteristics of the AMB pelitic nebulites with these experimental results suggests that these lithologies are the product of two melting events. In a first stage, the tonalitic gneisses underwent a hydrated melting. As the water was totally consumed, a subsequent dehydration melting event took place. The final result was the generation of granodioritic melts (El-Biad, 2000).

7.3. Basic magmatism

The starting material used to determine the origin of the syn-metamorphic basic magmatism in the CD of the AMB was a non-accumulated norite. This sample is representative of a primitive magma. Its typical mineral assemblage is ortopyroxene, clinopyroxene and plagioclase. The experiments were carried out at temperatures between 1100 and 1200ºC, and pressure conditions of 6, 10 and 14 kbar. For all the considered pressure conditions, the proportions of clinopyroxene, ortopyroxene and plagioclase decrease with the increase of temperature. The composition of the obtained melts was noritic with boninitic affinity (El-Hmidi, 2000). The experimental results also include a determination of the P-T conditions for the origin of the parental melt of the norites. These conditions are 1150ºC and 10 kbar (El-Hmidi, 2000). Both the geological and the experimental observations suggest that the sources of the basic magmatism (boninitic) in the CD of the AMB included two distinct components. One of these components was a metasomatic fluid released from the subducting oceanic slab, and the other component was located in the mantle wedge of the upper plate (El-Hmidi, 2000).

8. Tectono-metamorphic evolution of the AMB

The contact between the OMZ and the SPZ is depicted by the AMB, a HT/LP metamorphic belt of no more than a few km wide and more than 100 km long. The main features of the central sector of this belt have been exposed throughout the present contribution and are summarised below:

1.- The existence of a linear belt of oceanic (T-MORB affinities) metabasites with a LP inverted metamorphic gradient due to the superposition of two metamorphic events. OD-M_1 consisted in a HT/LP (amphibolite to granulite facies transition) event related to a non-coaxial shear deformation (OD-D_1) that gave place to a SW verging thrusting with a minor sinistral component. Both the metamorphism and the deformation of this first stage were more intense towards the structural top of the metabasitic pile. OD-M_1 shows an age gradient, in such a way that older ages have been obtained towards the west. OD-M_2 was a retrograde (low amphibolite to greenschists facies transition) metamorphic event that affected only to the lower half of the metabasitic pile. Related to OD-M_2, a mylonitic deformation took place in the SISZ, a transpressive shear zone that produced shortening normal to the shear plane, accompanied by a sinistral non-coaxial component.

2.- The CD was affected by, at least, four ductile deformation events. CD-D_1 could have generated recumbent km-scale folds with SW vergence. CD-D_2 produced an axial vertical shortening due to a main pure shear component accompanied by a subordinated simple shear component that was predominant within discrete normal shear zones. This deformation event, consistent with an extensional collapse or a gravity spreading, gave place to the main metamorphic foliation of the CD and obliterated, almost completely, the structures formed during CD-D_1. This second deformation stage was contemporary with a HT/LP metamorphic event, which followed a clock-wise path with a nearly isobaric heating, and gave place to several migmatitic complexes. CD-D_3 generated the gentle folding of previous structures. Finally, CD-D_4 gave place to thrusts with a top-to-the SSW sense of movement, accompanied by thrust accommodation folds. CD-D_4 is kinematically comparable to OD-D_3, which gave place to the Calabazares shear zone affecting the top of the Acebuches metabasites.

3.- The metamorphic gradient observed in the AMB is symmetric with respect to the contact between the OD and the CD. This fact, taking into account the north-dipping attitude of the CD, indicates that the CD shows a metamorphic normal gradient. The highest temperatures recorded in the CD are around 1000 ºC whereas those of the OD are under 800 ºC. Therefore, it seems likely that the OD was

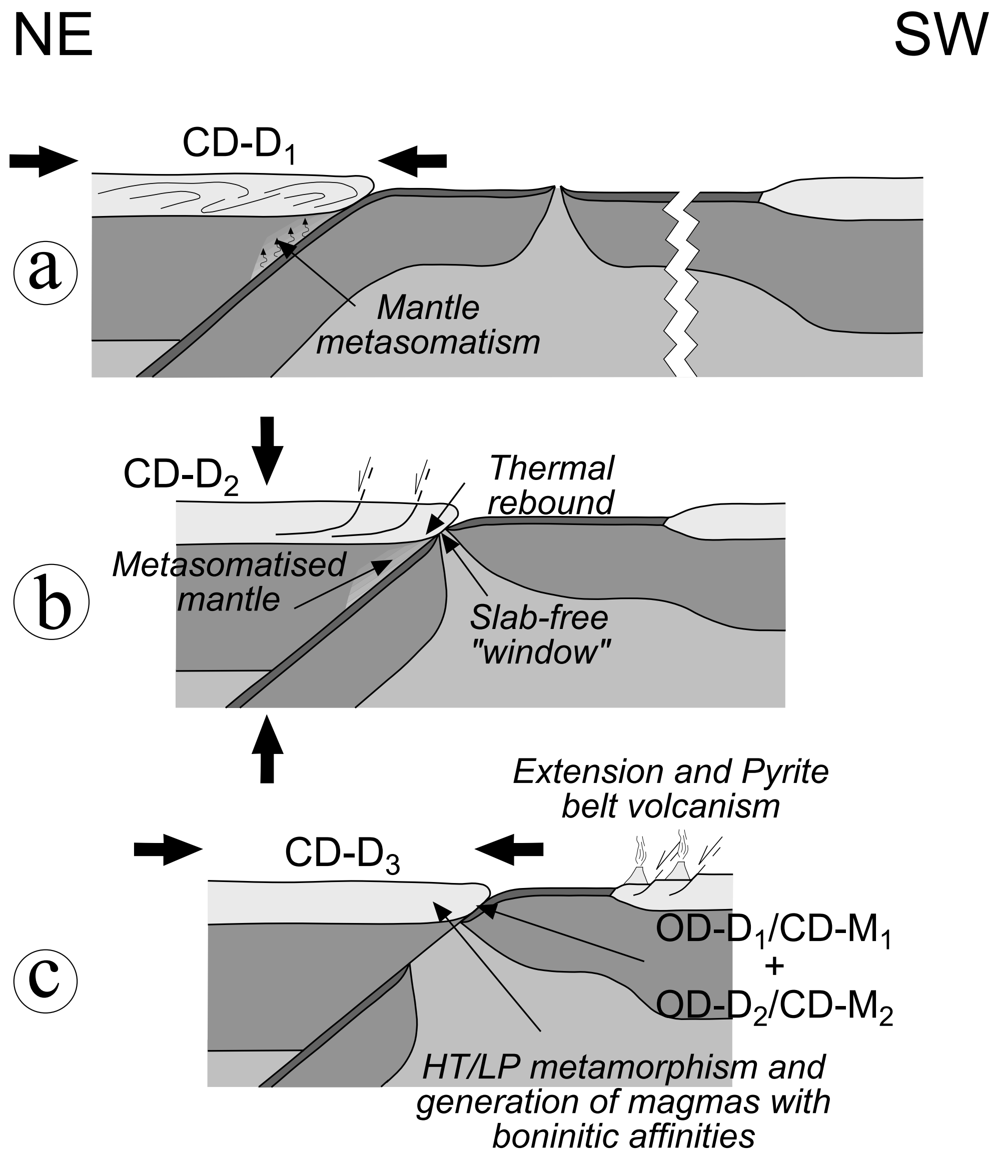

Fig. 15.- Tectonic model proposed for the variscan evolution of the AMB (simplified from Díaz Azpiroz *et al*., 2003a). Geographic references are as in present (with no scales). **a**) After the formation of an oceanic ridge between the Iberian autochton and the alochtonous South-Portuguese plate, the oceanic leading plate is subducted beneath the Iberian plate. Metasomatism of part of the lithospheric mantle and CD-D_1 developed. **b**) Subduction of the ridge as a consequence of the triple junction migration. The opening of a "slab-free window" gave place to a thermal rebound that heated up the base of the continental crust and produced magmas with boninitic affinities. At the same time extensional structures (CD-D_2) were generated. **c**) Inverted HT/LP metamorphism and related shear deformation (OD-D_1) affecting the trailing oceanic plate. The accretion of the top of this plate to the base of the continental margin provoked the migration of the subduction plane to the SISZ. The continental margin, together with the Acebuches metabasites, overthrusted the rest of the oceanic plate as well as the accretionary prism through the SISZ (OD-D_2). In the CD, upright folds generated (CD-D_3).

Fig. 15.- Modelo tectónico propuesto para la evolución varisca de la AMB (simplificado de Díaz Azpiroz *et al*., 2003a). Las referencias geográficas son las actuales (sin escala). **a**) Después de la formación de una dorsal oceánica entre el autóctono Ibérico y la placa alóctona Sudportuguesa, la placa oceánica delantera es subducida bajo la placa Ibérica. Durante este proceso se produce el metasomatismo de parte del manto litosférico, así como la fase CD-D_1. **b**) Subducción de la dorsal como consecuencia de la migración de la unión triple. La apertura de una ventana litosférica dio lugar a un rebote térmico que calentó la base de la corteza continental y produjo magmas de afinidad boninítica. Al mismo tiempo se generaron estructuras extensionales (CD-D_2). **c**) La placa oceánica trasera se ve afectada por un metamorfismo AT/BP invertido y una deformación cizallante (OD-D_1). La acreción del techo de esta placa a la base del margen continental provocó la migración del plano de subducción hacia la SISZ. El margen continental, junto con las metabasitas de Acebuches, cabalgaron sobre el resto de la placa oceánica y el prisma de acreción mediante la SISZ (OD-D_2). En el CD se generaron pliegues verticales (CD-D_3).

heated up by the CD.

4.- All the thermal events of the AMB took place during the Variscan orogeny, in the Visean to Namurian period. Most ages reported from the CD are older than those of the oceanic amphibolites located in the same traverse.

5.- The calc-magnesian series of the CD, characterised by fine-grained amphibolitic dikes associated with calc-silicate rocks and marbles, have been interpreted as derived from a bi-modal volcano-sedimentary series related to the opening of a continental rifting.

6.- The presence of syn- to post-tectonic noritic intrusions with high-Mg andesite (boninitic affinity) composition, possibly related to partial melting of a shallow mantle wedge (cf. Duncan and Green, 1987; Klingenberg and Kushiro, 1994).

According to the mentioned features, different tectonic models have been suggested (*e.g.*, Abalos *et al.*, 1991; Crespo-Blanc and Orozco, 1991; Bard, 1992; Quesada *et al.*, 1994; Giese *et al.*, 1994b). In this paper a model, based on that proposed by Castro *et al.* (1996a, b), is presented to explain the tectonic evolution of the AMB (Fig. 15):

1.- Continental rifting, oceanic ridge and passive margin stages (Cambrian-Silurian). The oceanic basalt with T-MORB affinities was generated at the oceanic ridge, and constitutes the parental rock of the Acebuches metabasites.

2.- Subduction of the leading oceanic plate (Devonian?). The oceanic lithosphere that evolved towards the NE of the ridge completely subducted beneath the northern continental margin (the current CD). The convergent motion between plates led to shortening in the CD, which can be identified as the CD-D_1 phase (Fig. 15a). The presence of calc-alkaline magmatism in the western and central parts of the Ossa-Morena Zone supports a subduction beneath the Iberian autochthonous terrain (Quesada, 1991)

3.- Ridge subduction (Tournaisean-Visean). Once the leading plate was consumed, the oceanic ridge intersected the subduction zone generating a TTR triple junction and a related slab-free window (Fig. 15b). This phenomenon provoked the upwelling of the underlying astenosphere and a subsequent thermal rebound. This anomalous high temperature in shallow deeps of the continental crust gave rise to a HT/LP metamorphic event, as well as the partial melting of a metasomatised mantle wedge, which produced magmas with boninitic affinities. Absolute age determinations suggest that the triple junction migrated along the southern continental edge towards the east, which generated a long and narrow high-grade metamorphic belt (namely, the AMB).

The subduction of the oceanic ridge induced a relaxation of the compressive stress (see Platt, 1986; Thorkelson, 1996). Although the cortical thickening was not significant, the tectonic scenario was in some way favourable for an extensional collapse, during which an axial shortening took place (CD-D_2).

4.- Subduction of the trailing plate (Visean-Namurian): Once the triple junction was passing by, subduction of the trailing plate begun beneath the northern continental edge, whose rocks had been previously heated up. Therefore, the rocks located at the upper levels of the oceanic sheet were heated up by the CD, giving rise to the currently observed inverted metamorphic gradient of the Acebuches series.

This subduction process induced a NNE-SSW oriented compression that affected both the continental (CD-D_3) and the oceanic (OD-D_1) domains (Fig. 15c).

5.- Emplacement of the Acebuches metabasites (Namurian). As the temperature of the oceanic subducting slab rose, the rocks located at the upper levels become dehydrated and were accreted to the base of the continental margin. The process involved the downgoing migration of the subduction plane towards more hydrated levels that favoured the shear deformation (Fig. 15c). Through this plane (namely, the current SISZ), the continental plate plus the upper levels of the oceanic slab overthrusted the rest of the oceanic lithosphere (OD-D_2 phase), which was totally subducted, as well as the accretionary prism (the Pulo do Lobo terrain). This process produced the uplift rate required to preserve the inverted metamorphic gradient (see Peacock, 1987).

6.- Continental collision (Namurian-Westphalian). Once the trailing plate was completely consumed, the southern continental margin (the current SPZ) subducted beneath the northern continental margin and, subsequently, both continental plates collided. This continental collision took place in a transpressive regime (Crespo-Blanc and Orozco, 1988; 1991; Abalos *et al.*, 1991; Bard, 1992; Giese *et al.*, 1994b) and promoted the last ductile deformation phases recorded in the AMB (CD-D_4 and OD-D_3) that generated km scale antiforms and inverse shear zones with SSW vergence.

Acknowledgements

Constructive reviews by J. Abati and C. Casquet improved the manuscript. The results presented in this work are a part of the Ph.D. Theses of Manuel Díaz Azpiroz, Hassan El-Hmidi and Mohammed El-Biad. Financial support from projects PB91-0600 and PB94-1085 (Spanish Science Comission, CICYT-DGES) and the University of Huelva is gratefully acknowledged.

References

Abalos, B., Gil Ibarguchi, I., Eguiluz, L. (1991): Structural and metamorphic evolution of the Almadén de la Plata Core (Sevilla, Spain) in relation to syn-metamorphic shear between the Ossa Morena and South Portuguese zones of the Iberian Variscan fold belt. *Tectonophysics*, 191: 365-387.

Apalategui, O., Barranco, E., Contreras, F., Delgado, M., Roldán, F. J., Quesada, C. (1983): Hoja geológica núm. 916 (Aroche). *Mapa Geológico de España E. 1:50. 000.* I.G.M.E., Madrid.

Apalategui, D., Barranco, E., Contreras, F., Delgado, M., Roldan, F. J. (1984): Hoja geológica núm. 917 (Aracena). *Mapa Geológico de España E. 1:50. 000.* I.G.M.E., Madrid.

Apalategui, O., Contreras, F., Eguiluz, L. (1990): Hoja geológica núm. 918 (Santa Olalla del Cala). *Mapa Geológico de España E. 1:50. 000.* I.G.M.E., Madrid.

Apraiz, A. (1998): *Geología de los macizos de Lora del Río y Valuengo (Zona de Ossa Morena): Evolución tectonometamórfica y significado geodinámico*. Tesis Doctoral, Universidad del País Vasco, 500 p.

Bard, J. P. (1967a): Sous-fácies ortopyroxene-hornblende dans la catazone de la bande métamorphique d´Aracena (Huelva), Espagne. *Comptes Rendus de l'Academie de Science de Paris*, 264: 2869-2872.

Bard, J. P. (1967b): Tectoniques superposeés et métamorphisme dans la bande crisallophyllienne d´Aracena (province de Huelva, Espagne). *Bulletin de la Societé geologique de France*, 128: 111-128.

Bard, J. P. (1969): *Le métamorphisme régional progressif de Sierra de Aracena en Andalousie occidentale (Espagne)*. Thèse d' Etat, Université de Montpellier, 397 p.

Bard, J. P. (1970): Composition of Hornblendes formed during the Hercynian progressive metamorphism of the Aracena Metamorphic Belt (SW Spain). *Contributions to Mineralogy and Petrology*, 28: 117-134.

Bard, J. P. (1977): Signification tectonique des métatholeiites d'affinité abyssale de la ceinture métamorphique de basse pression d'Aracena (Huelva, Espagne). *Bulletin de la Societé geologique de France*, XIX (2): 385-393.

Bard, J. P., Moine, B. (1979): Acebuches amphibolites in the Aracena hercynian metamorphic belt (southwest Spain): Geochemical variations and basaltic affinities. *Lithos*, 12: 271-282.

Bard, J. P. (1992): Les complexes intrusifs acide-basique calcoalcalins de la chaîne varisque sud-ibérique et leurs liaisons avec les grands cisaillements transpressifs de Badajoz-Cordue et de la zone sud-ibérique: proposition de modèles géodynamiques impliquant des processus de subduction continentale. *Comptes Rendus de l'Academie de Science de Paris*, 314: 711-716.

Barranco, E., Contreras, F., Roldán, F. J. (1983): Hoja geológica núm. 915 (Rosal de la Frontera). *Mapa Geológico de España E. 1:50. 000.* I. G. M. E., Madrid.

Batchelor, R. A., Bowden, P. (1985): Petrogenetic interpretation of granitoid rock series using multicationic parameter. *Chemical Geology*, 48: 43-55.

Berman, R. G. (1991): Thermobarometry using multiequilibrium calculations: a new technique with petrologic applications. *Canadian Mineralogist*, 29: 833-855.

Berthé, D., Choukroune, P., Jegouzo, P. (1979): Orthogneiss, mylonite and non coaxial deformation of granites: the example of South Armorican Shear Zone. *Journal of Structural Geology*, 1: 31-42.

Blundy, J. D., Holland, T. J. B. (1990): Calcic amphibole equilibria and a new amphibole-plagioclase geothermometer. *Contributions to Mineralogy and Petrology*, 104: 208-224.

Bowman, J. R. (1998): Stable-isotope systematic of skarns. In: D. R. Lentz (ed.): *Mineralized Intrusion-Related Skarn System*. Mineral Association of Canada Short Course Series: 99-145.

Cameron, W. E., Mcculloch, M. T., Walker, D. A. (1983): Boninite petrogenesis: chemical and Nd-Sr isotopic constraints. *Earth and Planetary Science Letters*, 65: 75-89.

Castro, A., Fernández, C., De La Rosa, J. D., Moreno-Ventas, I., El-Hmidi, H., El-Biad, M., Bergamin, J. F., Sánchez, N. (1996a): Triple-junction migration during Paleozoic Plate convergence: the Aracena metamorphic belt, Hercynian massif, Spain. *Geologische Rundschau*, 85: 108-185.

Castro, A., Fernández, C., De La Rosa, J. D., Moreno-Ventas, I., Rogers, G. (1996b): Significance of MORB-derived Amphibolites from the Aracena Metamorphic Belt, Southwest Spain. *Journal of Petrology*, 37: 235-260.

Castro, A., Fernández, C., El-Hmidi, H., El-Biad, M., Díaz, M., De La Rosa, J. D., Stuart, F. (1999a): Age constraints to the relationships between magmatism, metamorphism and tectonism in the Aracena metamorphic belt, southern Spain. *International Journal of Earth Sciences*, 88: 26-37.

Castro A., Patiño Douce A. E., Corretgé L. G., De La Rosa J. D., El-Biad M., El-Hmidi H. (1999b): Origin of peraluminous granites and granodiorites, Iberian Massif, Spain: an experimental test of granite petrogenesis. *Contributions to Mineralogy and Petrology*, 135: 255-276.

Chacón Muñoz, H., Fernández, C., Fernández-Caliani, J. C., Moreno-Ventas, I. (2001): Modelo de orientación cristalográfica preferente de dolomita, olivino y flogopita en mármoles de alta temperatura de la banda metamórfica de Aracena. *XXI^{a} Reunión anual de la Sociedad Española de Mineralogía*, Málaga, 24A: 15-16.

Crawford, A. J., Beccaluva, L., Serri, G. (1981): Tectono-magmatic evolution of the West Philippine-Mariana region and the origin of boninites. *Earth and Planetary Science Letters*, 54: 346-356.

Crawford, A. J., Falloon, T. J., Green, D. H. (1989): Classification, petrogenesis and tectonic setting of boninites. In: A. J. Crawford (ed.): *Boninites and Related Rocks*, Unwin Hyman, London: 1-49

Crespo-Blanc, A. (1987): El macizo de Aracena (Macizo Ibérico meridional): Propuesta de división sobre la base de nuevos datos estructurales y petrográficos. *Boletín Geológico y Minero*, 98: 507-515.

Crespo-Blanc, A. (1991): *Evolución geotectónica del contacto entre la Zona de Ossa Morena y la zona Sudportuguesa en las sierras de Aracena y Aroche (Macizo Ibérico Meridional): Un* *contacto mayor en la cadena Hercínica Europea*. Tesis Doctoral, Universidad de Granada: 327 p.

Crespo-Blanc, A., Orozco, M. (1988): The Southern Iberian Shear Zone: A major boundary in the Hercynian folded belt. *Tectonophysics*, 148: 221-227.

Crespo-Blanc, A., Orozco, M. (1991): The boundary between the Ossa Morena and Southportuguese Zones (Southern Iberian Massif): a major suture in the European Hercynian Chain. *Geologische Rundschau*, 80: 691-702.

Dallmeyer, R. D., Fonseca, P. E., Quesada, C., Ribeiro, A. (1993): $^{40}Ar/^{39}Ar$ mineral age constraints for the tectonothermal evolution of a Variscan suture in southwest Iberia. *Tectonophysics*, 222: 177-194.

Díaz Azpiroz, M. (2001): *Evolución tectono-metamórfica del dominio de alto grado de la banda metamórfica de Aracena*. Tesis Doctoral, Universidad de Huelva: 556 p.

Díaz Azpiroz, M., Fernández Rodríguez, C. (2000): Análisis de la variación del tamaño de grano en las metabasitas de la serie de Acebuches (Macizo Ibérico meridional). *Geotemas*, 1: 229-231.

Díaz Azpiroz, M., Fernández, C. (2001): Análisis estructural de los mármoles de la banda metamórfica de Aracena (Macizo Ibérico meridional). Implicaciones tectónicas regionales. *Geogaceta*, 31:119-122.

Díaz Azpiroz, M., Fernández, C. (2003): Characterization of tectono-metamorphic events using crystal size distribution (CSD) diagrams. A case study from the Acebuches metabasites (SW Spain). *Journal of Structural Geology*, 25: 935-947.

Díaz, M., Fernández, C., Castro, A. (1997): Structural and metamorphic characteristics of the Acebuches Amphibolites (SW Iberian massif). A model for the preservation of the upper oceanic crust in sutures resulting from triple junction evolution. *Terra Nova*, 9: p. 384.

Díaz Azpiroz, M., Castro, A., Fernández, C. (2001): Caracterización petrológica y geoquímica de los granitos metaluminosos tardíos del dominio continental de la banda metamórfica de Aracena (Macizo Ibérico meridional). *Geogaceta*, 30: 41-44.

Díaz Azpiroz, M., Fernández, C., Castro, A. (2002) El evento de fusión parcial en el dominio continental de la banda metamórfica de Aracena (Macizo Ibérico meridional): condicionantes estructurales, geoquímicos e isotópicos. *Revista de la Sociedad Geológica de España*, 15: 27-39.

Díaz Azpiroz, M., Fernández, C., Castro, A. (2003a): TTR triple junction evolution during plate convergence in the southern branch of the European Variscan Orogen. *Geophysical Research Abstracts*, vol 5.

Díaz Azpiroz, M., Fernández, C., Castro, A. (2003b): Estructura y evolución tectónica del dominio continental de la banda metamórfica de Aracena (Macizo Ibérico Meridional) *Revista de la Sociedad Geológica de España*, 16: 167-184.

Duncan, R. A., Green, R. H. (1987): The genesis of refractory melts in the formation of oceanic crust. *Contributions to Mineralogy and Petrology*. 96: 326-342.

Dupuy, C., Dostal, J., Bard, J. P. (1979): Trace element geochemistry of paleozoic amphibolites from SW Spain. *Tschermaks Mineralogische und Petrographische Mitteilungen*, 26: 87-93.

Eden, C. (1991): *Tectonostratigraphic analysis of the northern extent of the oceanic exotic terrane, northwestern Huelva province, Spain*. Ph. D. Thesis, University of Southampton: 223 p.

El-Biad, M. (2000): *Generación de granitoides en ambientes geológicamente contrastados del Macizo Ibérico. Limitaciones experimentales entre 2 y 15 kbar*. Tesis Doctoral, Universidad de Huelva: 310 p.

El-Biad, M., El-Hmidi, H., Díaz, M., Castro, A., Fernández, C. (1997): Dating high temperature events in the continental domain of the Aracena Metamorphic Belt (SW Iberian Massif). An evidence for a local metamorphic peak related to ridge subduction. *Terra Nova*, 9: p. 493.

El-Hmidi, H. (2000): *Petrología y geoquímica de los sistemas andesíticos ricos en Mg: estudio petrológico y experimental de las noritas de la Banda Metamórfica de Aracena, SO de España*. Tesis Doctoral, Universidad de Huelva: 239 p.

Falloon, T. J., Green, D. H., Mcculloch, M. T. (1989): Petrogenesis of high-Mg and associated lavas from the northern Tonga trench. In: J. A. Crawford (ed.) *Boninites and related rocks.* Unwin Hyman, London: 357-395.

Fernández-Caliani, J. C., Miras, A., Moreno-Ventas, I., Requena, A. (2001): Las rocas calcosilicatadas del extremo occidental de la banda metamórfica de Aracena (Huelva). Interés mineralógico y petrogenético. *XXI^a Reunión anual de la Sociedad Española de Mineralogía*, Málaga, 24A: 125-126.

Fernández-Caliani, J. C., Moreno-Ventas, I., Miras, A., Requena, A. (2002): Nódulos de wollastonita en mármoles de alta temperatura de la banda metamórfica de Aracena (Huelva) ¿Origen metamórfico o metasomático? *XXI^a Reunión anual de la Sociedad Española de Mineralogía*, Málaga, 25A: 31-32.

Fonseca, P., Ribeiro, A. (1993): Tectonics of the Beja-Acebuches ophiolite: a major suture in the Iberian Variscan Foldbelt. *Geologische Rundschhau*, 82: 440-447.

Giese, U., Walter, R., Von Winterfeld, C. (1994a): Geology of the southern Iberian Meseta II. The Aracena Metamorphic Belt between Almonaster La Real and Valdelarco, Huelva province (SW Spain). *Neues Jahrbuch für Geology Paläontology Abhandlungen*, 192: 333-360.

Giese, U., Von Hoegen, R., Hoymann, K. H., Kramm, U., Walter, R. (1994b): The Palaeozoic evolution of the Ossa - Morena zone and its boundary to the South Portuguese zone in SW Spain: Geological constraints and geodynamic interpretation of a suture in the Iberian Variscan orogen. *Neues Jahrbuch für Geology Paläontology Abhandlungen*, 192: 383-412.

Grapes, R. H., Graham, C. M. (1978): The actinolite-hornblende series in metabasites and the so-called miscibility gap: A review. *Lithos*, 11: 85-97.

Gregory, R. T., Taylor, H. P. (1981): An oxygen isotope profile in a section of Cretaceous oceanic crust, Samail ophiolite, Oman: Evidence for $\partial^{18}O$ buffering of the oceans by deep (5 km) sea water-hydrothermal circulation at mid-ocean ridges. *Journal of Geophysical Research*, 86: 2737-2755.

Hickey, R. L., Frey, F. A. (1982): Geochemical characteristics of boninite series volcanics: implications for the source. *Geochimica et Cosmochimica Acta*, 46: 2099-2115.

Holland, T. J. B., Blundy, J. D. (1994): Non-ideal interactions in calcic amphiboles and their bearing on amphibole-plagioclase thermometry. *Contributions to Mineralogy and Petrology*, 116: 433-447.

Hynes, A. (1982): A comparison of amphiboles from medium-low pressure metabasites. *Contributions to Mineralogy and Petrology*, 81: 119-125.

Klingenberg, B. M. E. T, Kushiro, I. (1994): Melting of a chromite-bearing harzburgite and generation of boninitic melts at low pressures under controlled oxygen fugacity. *Lithos*, 37: 1-16.

Kuehner, S. M. (1986): *Mafic dykes of the East Antarctic Shield, experimental, geochemical and petrological studies focusing on the Proterozoic evolution of the crust and mantle*. Ph. D. Thesis, University of Tasmania.

Kushiro, I., Shono, S., Akimoto, I. (1968): Melting of peridotite nodule at high pressure and high water pressures. *Journal of Geophysical Research*, 73: 6023-6029.

La Roche, H. D., Leterrier, J., Grande Claude, P., Marchal, M. (1980): A classification of volcanic and plutonic rocks using R1-R2 diagrams and major element analyses-its relationships and current nomenclature. *Chemical Geology*, 29: 183-210.

Laird, J. (1980): Phase equilibria in mafic schists from Vermont. *Journal of Petrology*, 21: 1-37.

Laird, J., Albee, A. L. (1981): Pressure, temperature and time indicators in mafic schist: their application to reconstructing the polimetamorphic history of Vermont. *American Journal of Science*, 281: 127-175.

Lin, S., Jiang, D., Williams, P. F. (1998): Transpression (or transtension) zones of triclinic symmetry: natural example and theoretical modelling. In: R. E. Holdsworth, R. A. Strachan, J. F. Dewey (eds.): *Continental Transpression and Transtension Tectonics*. Geological Society Special Publication, 135: 41-57.

López, S., Castro, A. (2001): Determination of the fluid-absent solidus and supersolidus phase relationship of MORB-derived amphibolites in the range 4-14 kbar. *American Mineralogist*, 86: 1396-1403.

Martin, H. (1999): Adakitic magmas: modern analogues of Archean granitoids. *Lithos*, 46: 411-429.

Maruyama, S., Suzuki, K., Liou, J. G. (1983): Greenschist-amphibolite transition equilibria at low pressures. *Journal of Petrology*, 24: 583-604.

Mcculloch, M. T., Gregory, R., Wasserburg, G. J., Taylor, H. P. (1980): A neodymium, strontium, and oxygen isotopic study of the cretaceous Samail ophiolite and implications for the petrogenesis and seawater-hydrothermal alteration of oceanic crust. *Earth and Planetary Science Letters*, 46: 201-211.

Mcculloch, T. M., Cameron, W. E. (1983): Nd-Sr isotopic study of primitive lavas from the Troodos Ophiolite, Cyprus: evidence for a subduction-related setting. *Geology*, 11: 727-731.

Meijer, A. (1980): Primitive arc volcanism and a boninite series: example from W-Pacific Island arcs. In: D. F. Hayes (ed.): *The Tectonic and Geologic Evolution of southeast Asian seas and islands*. AGU Monographs, 23: 269-282.

Miyashiro, A. (1973): *Metamorphism and metamorphic belts*. 492 p., George Allen and Unwin Ltd., London.

Moody, J. B. M. D., Jenkins, J. E. (1983): Experimental characterization of the greenschist/amphibolite boundary in mafic systems. *American Journal of Science*, 283: 48-92.

Moreno-Ventas, I., Fernández-Caliani, J. C., Miras, A., Requena, A. (2002): Generación de diques compuestos por fenómenos de asimilación y metasomatismo en la banda metamórfica de Aracena (Zona Ossa Morena). *XXI^a^ Reunión anual de la Sociedad Española de Mineralogía*, Málaga, 25A: 69-70.

Mullen, E. D. (1983): $MnO/TiO_2/P_2O_5$: a minor element discriminant for basaltic rocks of oceanic environments and its implications for petrogenesis. *Earth Planetary Science Letters*, 62: 53-62.

Munhá, J. M., Oliveira, J. T., Ribeiro, A., Oliveira, V., Quesada, C., Kerrich, R. (1986): Beja-Acebuches ophiolite: Characterization and geodynamic significance. *Maleo*, 2: p. 30.

Nelson, D. R., Crawford, A. J., Mcculloch, M. T. (1984): Nd-Sr isotopic and geochemical systematics in Cambrian boninites and tholeiites from Victoria, Australia. *Contributions to Mineralogy and Petrology*, 88: 164-172.

Passchier, C. W., Trouw, R. A. J. (1996): *Microtectonics*. Springer-Verlag, Berlin: 289 p.

Patiño Douce, A. E., Johnston, A. D. (1991): Phase equilibria and melt productivity in the pelitic system: implications for the origin of peraluminous granitoids and aluminous granulites. *Contributions to Mineralogy and Petrology*, 107: 202-218.

Patiño Douce, A. E., Castro, A., El-Biad, M. (1997): Thermal evolution and tectonic implications of spinel-cordierite granulites from the Aracena Metamorphic Belt, Southwest Spain. *GAC/MAC Annual Meeting*, 22: p. A113.

Peacock, S. M. (1987): Creation and preservation of subduction-related inverted metamorphic gradients. *Journal of Geophysical Research*, 92: 12763-12781.

Pearce, J. A. (1983): The role of the sub-continental lithosphere in magma genesis at destructive plate margins. In: C. J. Hawkesworth, M. J. Norry (eds.): *Continental basalts and mantle xenoliths*: 230-249. Shiva, Nantwich.

Pearce, J. A., Harris, N., Tindle, A. G. (1984): Trace element discrimination diagrams for the tectonic interpretation of granitic rocks. *Journal of Petrology*, 25: 956-983.

Perchuk, L. L. (1991): Derivation of a thermodynamically consistent set of geothermometers and geobarometers for metamorphic and magmatic rocks. In: L. L. Perchuk (ed.): *Progress in Metamorphic and Magmatic Petrology*: 93-111. Cambridge University Press, Cambridge.

Perchuk, L. L., Lavrent'eva, I. V. (1983): Experimental investigations of exchange equilibria in the system cordierite-garnet-biotite. In: S. K. Saxena (ed.): *Kinetics and Equilibrium in Mineral Reactions*. Adv. Phys. Geochem., 3: 199-239, Springer-Verlag, New York.

Platt, J. P. (1986): Dynamics of orogenic wedges and the uplift of high-pressure metamorphic rocks. *Geological Society of America Bulletin*, 97: 1037-1053.

Ponce De León, M. I., Choukroune, P. (1980): Shear zones in the Iberian Arc. *Journal of Structural Geology*, 2: 63-68.

Quesada, C. (1991): Geological constraints on the Paleozoic tectonic evolution of tectonostratigraphic terranes in the Iberian Massif. *Tectonophysics*, 185: 225-245.

Quesada, C., Fonseca, P. E., Munhá, J., Oliveira, J. T., Ribeiro, A. (1994): The Beja-Acebuches Ophiolite (Southern Iberia Variscan fold belt): Geological characterization and geodynamic significance. *Boletín Geológico y Minero*, 105: 3-49.

Ramsay, J. G. (1967): *Folding and fracturing of rocks*. McGraw-Hill, London: 591 p.

Rodas, M., Luque, F. J., Barrenechea, J. F., Fernández-Caliani, J. C., Miras, A., Fernández Rodríguez, C. (2000): Graphite occurrences in the Low-Pressure/High-Temperature metamorphic belt of the Sierra de Aracena (Southern Iberian Massif). *Mineralogical Magazine*, 64: 801-814.

Rogers, N. W., Macleod, C. J., Murton, B. J. (1989): Petrogenesis of boninitic lavas from the Limassol Forest Complex, Cyprus. In: A. J. Crawford (ed.): *Boninites and Related Rocks*. Unwin Hyman, London: 288-313.

Rollinson, H. R. (1993): *Using Geochemical Data: Evaluation, presentation, interpretation*. Longman Scientific and Technical, New York: 352 p.

Saunders, A. D. (1984): The rare earth element characteristics of igneous rocks from the ocean basins. In: P. Henderson (ed.): *Rare Earth Element Geochemistry*. Elsevier, Amsterdam: 205-236.

Schermerhorn, J. L. G. (1971): An outline of the stratigraphy of the Iberian Pyrite Belt. *Boletín Geológico y Minero*, 82: 239-268.

Schmid, S. M., Casey, M. (1986): Complete fabric analysis of some commonly observed quartz c-axis patterns. *Geophysical Monographs*, 36: 263-286.

Spear, F. S. (1981): An experimental study of hornblende stability and compositional variability in amphibolite. *American Journal of Science*, 281: 697-734.

Spear, F. S. (1993): *Metamorphic phase equilibria and pressure-temperature-time paths*. Mineralogical Society of America, Washington, D. C.: 799 p.

Tatsumi, Y., Maruyama, S. (1989): Boninites and high-Mg andesites: tectonics and petrogenesis. In: A. J. Crawford (ed.): *Boninites and Related Rocks*: 50-71. Unwin Hyman, London.

Thiessen, R. L., Means, W. D. (1980): Classification of fold interference patterns: a reexamination. *Journal of Structural Geology*, 2: 311-316.

Thorkelson, D. J. (1996): Subduction of diverging plates and the principles of slab window formation. *Tectonophysics*, 255: 47-63.

Valley, J. W. (1985): Polymetamorphism in the Adirondacks: Wollastonite at contacts of shallowly intruded anorthosite. In: A. C. Tobi, J. L. R. Touret, (eds.): *The Deep Proterozoic Crust in the North Atlantic Provinces.* Riedel, New York: 217-236.